

## Lava flow hazard map of Piton de la Fournaise volcano

Magdalena Oryaëlle Chevrel<sup>1</sup>, Massimiliano Favalli<sup>2</sup>, Nicolas Villeneuve<sup>3,4,5</sup>, Andrew J. L. Harris<sup>1</sup>, Alessandro Fornaciai<sup>2</sup>, Nicole Richter<sup>3,5,6</sup>, Allan Derrien<sup>3,5</sup>, Patrice Boissier<sup>3,5</sup>, Andrea Di Muro<sup>3,5</sup>, Aline Peltier<sup>3,5</sup>

- 5 <sup>1</sup>Université Clermont Auvergne, CNRS, IRD, OPGC, Laboratoire Magmas et Volcans, F-63000 Clermont-Ferrand, France.  
<sup>2</sup>Istituto Nazionale di Geofisica e Vulcanologia (INGV), Via Battisti, 53, 56125 Pisa, Italy.  
<sup>3</sup>Université de Paris, Institut de physique du globe de Paris, CNRS, F-75005 Paris, France.  
<sup>4</sup>Université de La Réunion, Laboratoire Géosciences Réunion, F-97744 Saint-Denis, France.  
<sup>5</sup>Observatoire Volcanologique du Piton de la Fournaise, Institut de physique du globe de Paris, F-97418 La Plaine des Cafres,  
10 France.  
<sup>6</sup>Helmholtz Centre Potsdam, German Research Centre for Geosciences (GFZ), Telegrafenberg, Potsdam, 14473, Germany  
Correspondence to: Magdalena Oryaëlle Chevrel (oryaelle.chevrel@ird.fr)

**Abstract.** Piton de la Fournaise, situated on La Réunion Island (France), is one of the most active hot spot basaltic shield volcanoes worldwide, experiencing at least two eruptions per year since the establishment of the observatory in 1979. Eruptions  
15 are typically fissure-fed and form extensive lava flow fields. About 95 % of some ~250 historical events (since the first confidently dated eruption in 1708) have occurred inside an uninhabited horse-shoe shaped caldera (hereafter referred to as the Enclos), which is open to the ocean on its eastern side. Rarely (12 times since the 18<sup>th</sup> century), fissures have opened outside of the Enclos where housing units, population centers and infrastructure are at risk. In such a situation, lava flow hazard maps are a useful way of visualizing lava flow inundation probabilities over large areas. Here, we present the up-to-date lava  
20 flow hazard map for Piton de la Fournaise based on: i) vent distribution, ii) Java flow recurrence times, iii) statistics of lava flow lengths, and iv) simulations of lava flow paths using the DOWNFLOW stochastic numerical model. The map of the entire volcano highlights the spatial distribution probability of future lava flow invasion for the medium to long term (years to decades). It shows that the most probable location for future lava flow is within the Enclos (where there are areas with up to 12 % probability), a location visited by more than 100,000 visitors every year. Outside of the Enclos, probabilities reach 0.5 %  
25 along the active rift zones. Although lava flow hazard occurrence in inhabited areas is deemed to be very low (<0.1 %), it may be underestimated, as our study is only based on post-18<sup>th</sup> century records and neglects older events. We also provide a series of lava flow hazard maps inside the Enclos, computed on a multi-temporal (i.e., regularly updated) topography. Although hazard distribution remains broadly the same over time, some changes are noticed throughout the analyzed periods due to improved DEM resolution, the high frequency of eruptions that constantly modifies the topography, as well as the lava flow dimensional characteristics. The lava flow hazard map for Piton de la Fournaise presented here is reliable and trustworthy for long term hazard assessment, land use planning and management. Specific hazard maps for short term hazard assessment (e.g. for responding to volcanic crises) or considering the cycles of activity at the volcano and different event scenarios (i.e., events fed by different combinations of temporally evolving superficial and deep sources) are required for further assessment of

Supprimé: a

Supprimé: statistics of lava flow lengths, iii)

Supprimé: across multi-temporal (i.e., regularly updated) topography

Supprimé: A

Supprimé: (up to 12 %)

Supprimé: inundation

Supprimé: where

Supprimé: about

Supprimé: are present each

Supprimé: Hazard distribution changes throughout the analysis period due to the high frequency of eruptions that constantly modifies the vent opening distribution as well as the topography and the lava flow dimensional characteristics.

Supprimé: well-defined

Supprimé: and,

Supprimé: a

Supprimé: here

Supprimé: cycles of activity at the volcano.

Supprimé: to better assess

55 affected areas in the future – especially by atypical, but potentially extremely hazardous, large volume eruptions. At such an active site, our method supports the need for regular updates of DEMs and associated lava flow hazard maps if we are to be effective in keeping up-to-date with mitigating of the associated risks.

## 1 Introduction

Lava flow hazard maps represent the probability of inundation by a lava flow per unit area. Because such maps show areas that are at the highest risk, it is a fundamental tool in lava flow hazard mitigation and in guiding eruption response management. Lava flow hazard maps for basaltic volcanic centers have been previously produced for several highly active volcanoes including Mount Etna in Italy (Favalli et al., 2005; Favalli et al., 2011; Del Negro et al., 2013), Nyiragongo in the Democratic Republic of Congo (Chirico et al., 2009; Favalli et al., 2009), and Mount Cameroon in the Cameroon (Bonne et al., 2008; Favalli et al., 2012). They have also been produced for most ocean island basaltic shields including Mauna Loa and Kilauea on the island of Hawaii (Kauahikaua et al., 1998; Rowland et al. 2005), Lanzarote in the Canaries, Spain (Felpeto et al., 2001), Pico in the Azores, Portugal (Cappello et al., 2015), Fogo in Capo Verde (Richter et al. 2016), and Karthala in the Grande Comore (Mossoux et al., 2019). Having been active with an eruption every nine months since the beginning of the 20<sup>th</sup> century (Michon et al., 2013), producing such a map for Piton de la Fournaise (La Réunion, France) is a particularly pressing need. At the same time, the wealth of data for eruptive events at Piton de la Fournaise means that we can use this location as a case study to further test, develop and evolve methods for effective lava flow hazard map preparation at frequently active effusive centers.

Following widespread damage due to lava ingress into the town of Piton Sainte Rose in 1977, a volcano observatory the Observatoire Volcanologique du Piton de la Fournaise, (OVPF) managed by the Institut de Physique du Globe de Paris (IPGP) was established on Piton de la Fournaise in 1979. The objective was to install and maintain, in operational conditions, an adequate monitoring network to ensure surveillance of the volcano, thereby improving hazard mitigation. Today, the permanent monitoring network run by OVPF is one of the densest in the world, comprising more than 100 stations including seismometers, tiltmeters, extensometers, GNSS receivers, gas monitoring stations, cameras and weather stations. This network allows OVPF to detect eruption onset and provide early warning to authorities so that they can organize implementation of the nationally-mandated response plan to be followed by civil protection (the “ORSEC-DSO plan”), a plan which includes provision for evacuation of volcano visitors and resident populations if needed (Peltier et al., 2018, 2020). However, effective hazard management also requires preparation of hazard maps to guide mitigation measures and actions (Pallister et al., 2019). In this regard, an exhaustive database for eruptive events has been built by OVPF through their response to 77 eruptions between 1979 and 2019, all of which have been geophysically, petrographically and physically mapped and measured. The existence of such a database allows application of a robust empirical approach to hazard mapping and planning. Currently this database includes:

Supprimé: (

Supprimé: ,

Supprimé: ensure

Supprimé: and

Supprimé: (Pallister et al., 2019)

Supprimé:

Supprimé: (Pallister et al., 2019)

Supprimé:

- i) An exhaustive lava flow inventory based on detailed mapping over the period 1931–2019 (Derrien, 2019; Staudacher et al., 2016; OVPF database) coupled with lava flow dating (Albert et al., 2020) that allows estimation of ~~eruption and associated~~ lava flow recurrence times;
- ii) Three high-spatial (25 to 1 m) resolution Digital Elevation Models (DEMs) acquired in 1997, 2010 and 2016 (Arab-Sedze et al., 2014; Bretar et al., 2013; Derrien, 2019);
- iii) A ~~large database for vent distribution to allow robust calculation of the probability density function of future vent opening~~ (Favalli et al., 2009a).

Supprimé: the

Supprimé: complete

Supprimé:

Supprimé: (up to the end of 2019)

At Piton de la Fournaise, the impact of lava flow hazard has previously been studied by Villeneuve (2000) and Davoine and Saint-Marc (2016), and an initial lava flow hazard map was published in a national report in 2012 (Di Muro et al., 2012). This map is also mentioned in Nave et al. (2016). However, the hazard map was drafted based on a topography acquired in 1997, and between the publication of the national report in 2012 and the end of 2019, eighteen eruptions occurred resurfacing approximately 19 km<sup>2</sup> of land. Thus, regular reassessments of lava flow hazard at Piton de la Fournaise are needed to allow regular updates of maps in this highly active environment where topography is changing annually due to emplacement of new lava flow units. Mapping also needs to be flexible and reactive to the changing hazard situation as new vents and vent distributions become established (Favalli et al., 2009a). ~~The style (channelized versus tube-fed flow), magnitude (total volume erupted) and intensity (peak effusion rates) of effusive activity will also evolve to influence areas and lengths attained by lava flow fields (Walker, 1973; Keszthelyi and Self, 1998; Rowland et al., 2005; H Harris and Rowland, 2009).~~

Supprimé: , and t

Supprimé: .

Supprimé: volcano

Supprimé: s

Supprimé: magnitude and intensity of effusive volcano activity evolves

Supprimé: ; Keszthelyi and Self, 1998

Supprimé: a

Supprimé: this

To build a hazard map in such a dynamic environment we employed the DOWNFLOW code of Favalli et al. (2005), this being a stochastic model that allows quick, computationally efficient and flexible estimation of the most probable areas to be covered by lava flows (e.g., Favalli et al., 2009b, 2011; Richter et al., 2016). To apply DOWNFLOW, we need to calibrate it by obtaining the best-fit parameters to reproduce the area of lava flow coverage for selected flows. Building a hazard map, also involves calculation of the lava flow temporal recurrence intervals, as well as vent distributions (Favalli et al., 2009a). We here describe this methodology, step-by-step, and present the resulting up-to-date lava flow hazard map for Piton de la Fournaise. Additionally, we compare three hazard maps derived from three DEMs acquired in 1997, 2010 and 2016 to assess and discuss the effectiveness of this method, and the evolution of the hazard maps resulting from changes in the ~~the topography as expressed in the up-dated DEMs; as will be a common issue~~ at frequently active basaltic volcanoes. First, though, we present the ~~geological~~ setting and eruptive activity at Piton de la Fournaise so as to define the hazard and risk scenarios for this case type example.

Supprimé: the

Supprimé: the

Supprimé: occur,

Supprimé: DEMs; as will occur,

Supprimé: morphological

### 1.1. Geological setting

Supprimé: Morphological

La Réunion island is located in the western Indian Ocean, around 700 km east of Madagascar and 180 km southwest of Mauritius. The island is composed of two large shield volcanoes (Fig. 1a): Piton des Neiges, which is considered dormant, and Piton de la Fournaise which is one of the most active volcanoes in the world (Peltier et al., 2009; Roullet et al., 2012). The Piton de la Fournaise edifice is marked by a large horse-shoe shaped caldera, referred to hereafter by its local name “the Enclos”

(French for “enclosure”). The Enclos is a 8 km wide structure, which is open to the ocean to the east and is surrounded by cliffs of up 100 m high to the west, north and south (Fig. 1b). This ~~structure contains any active lava flow to the Enclos limits,~~ with the west to east slope guiding flow towards the ocean. Although it is commonly accepted that the Enclos is the most recent collapse structure at Piton de la Fournaise, its mechanisms of formation and respective ages are still debated. While it may have been formed by a series of collapses and successive landslides (Bachelery 1981; Merle et al., 2010; Michon and Saint-Ange, 2008; Merle and Lénat, 2003), it may also be the result of only landslides (Duffield et al., 1982; Gillot et al. 1994; Oehler et al. 2004, 2008). The upper part of the Enclos, whose western plateau is located at >1800-1700 m a.s.l., is recognized here as the caldera *sensu stricto* (Michon and Saint-Ange, 2008) and is named the Enclos Fouqué (EF) (Fig. 1b). It is a relatively flat plateau in the middle of which an asymmetric terminal shield has been built to reach an altitude of 2632 m a.s.l. and with slopes of between 15° (on the northern flank) and 30° (on the eastern flank). The top of the terminal shield is marked by a 1.1 × 0.8 km summit caldera (“Cratère Dolomieu”) that ~~has been formed by recurrent collapses, with the last collapse occurring in April 2007~~ (Michon et al., 2009; Staudacher et al., 2009; Derrien et al., 2020). To the west, Cratère Dolomieu coalesces with a smaller (0.38 × 0.23 km) crater (“Cratère Bory”). The eastern part of the Enclos, i.e., below 1800 m a.s.l., is divided into two areas (most probably formed by successive landslides; Michon and Saint-Ange, 2008) where the slopes are very steep (>30°), ~~a zone~~ hereafter named “Grandes Pentés” (French for “steep slopes”), and ~~a flatter coastal area, (< ° slopes)~~ hereafter named “Grand-Brûlé” (French for “widely-burned”; Fig. 1b).

**Supprimé:** morphology

**Supprimé:** last collapsed in

**Supprimé:** the

## 1.2 Effusive activity and risk

As observed on most basaltic shield volcanoes (Dvorak et al., 1983; Tilling and Dvorak, 1993; Walker, 1988), eruptions at Piton de la Fournaise are produced by dyke/sill propagation following preferential paths leading to the concentration of eruptive fissures within, tangential-to or radially-around the summit crater and along three main rift zones (Bachelery, 1981). At Piton de la Fournaise, there are three rift zones, the southeast rift zone (SERZ), the northeast rift zone (NERZ) and the north 120° rift zone (N120, Fig. 1b). ~~These rift zones are the preferential zones for opening of eruptive fractures, and consequently, are location where~~ effusive activity is ~~primarily initiated (cf. Dvorak & Dzurisin, 1993)~~. Two other zones with a high concentration of eruptive fissures have also been identified, these being the South Volcanic Zone (SVZ) and the Puy Raymond Volcanic Alignment (PRVA; Michon et al. 2015; Fig. 1b).

**Supprimé:** )

**Supprimé:** , and t

**Supprimé:** are

**Supprimé:** where

**Supprimé:** mainly

**Supprimé:** concentrated

**Supprimé:** Fig.1b

**Supprimé:** (Fig.1b)

**Supprimé:** expressed

**Supprimé:** , a distance of up to 12 km downslope

**Déplacé (insertion) [3]**

**Supprimé:** can be

**Supprimé:** (e.g., Harris et al., 2016; Rhéty et al., 2017; Soldati et al., 2018),

**Supprimé:** within the Enclos (Fig. 1b),

**Supprimé:** although

**Mis en forme :** Anglais (E.U.)

**Supprimé:** , as in 2007 (Staudacher et al., 2009).

**Code de champ modifié**

**Mis en forme :** Français

Eruptions are mainly effusive and fed by en-echelon fissure sets, with each fissure being a few meters to a few hundred meters long. Activity at the fissures tends to be Hawaiian to Strombolian in style, to feed lava flows that can extend all the way to the ocean (cf. Sect. 6). ~~Lava flows tend to be channel fed to feed extensive compound lava flow fields, and tubes can form during longer-lived eruptions~~ (Coppola et al., 2017; Rhéty et al., 2017; Soldati et al. 2018). ~~Lava composition is usually transitional, ranging from aphyric basalt to oceanite and midalkaline basalt (Albarède et al., 1997; Lénat et al., 2012), with eruption temperatures in the range 1150–1190 °C (e.g., Boivin and Bachelery, 2009; Harris et al., 2019; Di Muro et al., 2014). Lavas thus have a relatively low viscosity of the order of 10<sup>2</sup>–10<sup>4</sup> Pa s upon eruption~~ (Harris et al., 2015; Kolzenburg et al., 2018; Rhéty et al., 2017; Soldati et al., 2018; Villeneuve et al., 2008).

Most effusive eruptions at Piton de la Fournaise occur within the Enclos. This is part of La Réunion National Park and is uninhabited. However, being a major tourist attraction, the Enclos does receive more than one hundred thousand visitors per year. As a result the hiking trails in, and access roads to, the Enclos can receive heavy pedestrian and vehicular traffic where 129 000 hikers accessed the summit in 2011 (Derrien et al., 2018). The Enclos also hosts the island belt road (national road RN2) which crosses the Enclos for a length of 9.5 km from north to south, and is located at a distance of 800 m inland from the coast and at an altitude of 130-70 m a.s.l. (Fig. 1b). Being the only east coast line of communication, if cut, it severely impedes communications and travel between Eastern communities, in the south and the north of the island (Harris and Villeneuve, 2018). This road had an average of more than 4500 vehicles per day in 2014 (INSEE, 2014).

Based on an analysis of the records available since the first observation of activity in 1640, Villeneuve and Bachèlery (2006) estimated that 95 % of the historic eruptions have occurred in the Enclos Fouqué caldera. These are, hereafter, termed “proximal” eruptions as they are proximal to the terminal shield. Fissures and associated lava flows produced by these proximal eruptions may cut hiking trails and generate a risk for the visitors (Derrien et al., 2018), and necessitates evacuation and prohibition of access to the Enclos (Peltier et al., 2020). To ensure effective closure of the Enclos, a 2 m-high gate, located at the head of the trail descends a steep, narrow scallop in the Enclos cliff and allows hikers to reach the Enclos via the Pas de Bellecombe Jacob (Fig. 1). Fissures may also open on the Grandes Pentes or in the Grand-Brûlé, i.e., below 1800 m a.s.l. These are termed “distal” eruptions and these can flow over the RN2, as has been the case for eight eruptions since 1979 (Fig. 1b). Eruptions outside of the Enclos, called Hors Enclos eruptions – “hors” being French for outside, are high risk as fissures can open in or above inhabited areas near the coast, such as above the villages of Sainte-Rose and Saint-Philippe (Fig. 1b). They can also open in the inhabited highlands of the volcano, where there are the towns of La Plaine des Cafres and Plaines des Palmistes (Fig. 1b). For example, the eruption of April 1977, which was the first *Hors Enclos* eruption since 1800, caused evacuation of Piton Sainte-Rose, burnt down or damaged parts of 26 buildings (including houses, a church, the police station and a gas station) and buried part of the Sainte-Rose municipality (Kieffer et al., 1977, Vaxelaire, 2012). A second *Hors Enclos* eruption in March 1986 caused around 400,000 euros of damage to houses, household contents, agriculture, roads and utilities in the municipality of Sainte Phillippe (Bertile, 1987; Morin, 2012). In 1998 a third eruption occurred outside of the Enclos with lava moving down steep slope above the village Bois Blanc but flow fronts stopped before reaching the inhabited areas (Villeneuve et Bachèlery, 2006).

### 1.3 Cycles of effusive activity

At Piton de la Fournaise, spatiotemporal cycles in eruptive activity can be defined with typical periods of one year to slightly more than a decade. According to Peltier et al. (2009), Got et al. (2013) and Derrien (2019), superficial cycles are controlled by the evolution of the shallow (<2.5 km below the summit) stress field. These cycles have typical periods of one year to slightly more than a decade. A cycle typically starts with one or a few summit eruptions, followed by one or a few proximal eruptions (with vents opening on the terminal shield or at its base), and may end with a large-volume, distal eruption (“low flank”) taking place in the Grande Pentes or Grand Brûlé area, as was the case in 2007, or with an *Hors Enclos* eruption,

**Déplacé vers le haut [3]:** Lava flows can be channel fed (e.g., Harris et al., 2016; Rhéty et al., 2017; Soldati et al., 2018), to feed extensive compound lava flow fields within the Enclos (Fig. 1b), although tubes can form during longer-lived eruptions, as in 2007 (Staudacher et al., 2009). Lava composition is usually transitional, ranging from aphyric basalt to oceanite and midalkaline basalt (Albarède et al., 1997; Lénat et al., 2012), with eruption temperatures in the range 1150-1190 °C (e.g., Boivin and Bachèlery, 2009; Harris et al., 2019; Di Muro et al., 2014). Lavas thus have a relatively low viscosity of the order of  $10^2$ - $10^4$  Pa s upon eruption (Harris et al., 2016; Kolzenburg et al., 2018; Rhéty et al., 2017).

**Supprimé:** The average volume of lava emitted per eruption between 1970 and 2007 was about  $10 \times 10^6$  m<sup>3</sup> (Peltier et al., 2009). In 2007, activity was punctuated by a low-elevation flank (590 m a. s. l.) event in the Enclos, during which 140 to  $240 \times 10^6$  m<sup>3</sup> of lava was erupted in 30 days (Roult et al., 2012; Staudacher et al., 2009). **Supprimé:**

**Supprimé:** about

**Supprimé:** (e.g.,

**Supprimé:** according to

**Supprimé:** (

**Supprimé:** at a

**Supprimé:** This is the island belt road and,

**Supprimé:** i

**Supprimé:** severely

**Supprimé:** in the

**Supprimé:**

**Supprimé:** .

**Supprimé:** analyses

**Supprimé:** (i.e., above 1800 m a.s.l.)

**Supprimé:** closure of

**Supprimé:** i

**Supprimé:** cut

**Supprimé:** termed

**Supprimé:** they

**Supprimé:** on the

**Supprimé:** high

**Supprimé:** from

**Supprimé:** the location and frequency of effusive activity is ... [2]

**Supprimé:** the stress field at Piton de la Fournaise can follow

**Supprimé:** that

**Supprimé:** These cycles

**Supprimé:** at the summit

**Supprimé:** . They may

**Supprimé:** s

**Supprimé:** at a distance of more than 4 km from the summit

as it was the case for the cycle that ended in 1977. In addition to these superficial cycles, lava composition seems to be affected by cyclic changes in the “fertility” of the source magma as observed since 1930, the date since which the petrology of the volcanic products has been well documented (Vlastélic et al., 2018). These deep source-related cycles are typically of longer

305 duration (20–30 years) than superficial cycles. They are characterized by a continuous increase of source fertility until reaching a maxima. This peak is followed by a continuous decrease in source fertility, until a minima is reached which marks the end of a cycle and the beginning of a new one (Vlastélic et al., 2018). High-volume distal eruptions associated with pit-crater collapse (cf Walker 1988) as in 1931-35, 1961, 1986 and 2007, have happened at the three-quarters of a compositionally defined (“deep-seated”) cycles, just after the peak of source fertility (Derrien, 2019).

310 The average volume of lava emitted per eruption between 1970 and 2007 was about  $10 \times 10^6 \text{ m}^3$  (Peltier et al., 2009). In 2007, when the activity was punctuated by a low-elevation (590 m a. s. l.) flank event in the Enclos,  $140 \text{ to } 240 \times 10^6 \text{ m}^3$  of lava was erupted in 30 days (Derrien, 2019; Roult et al., 2012; Staudacher et al., 2009). Historically the 2007 event has been, volumetrically, the largest single effusive event witnessed at Piton de la Fournaise. Through end of 2019, the March-April 2007 eruption has been followed by a further 25 more “typical” eruptions (highly frequent), each with a typical volume of  $5 \times$

315  $10^6 \text{ m}^3$  and being fed from vents at higher ( $> 1700 \text{ m a.s.l.}$ ) altitudes (OVVF reports ISSN 2610-5101). These spatiotemporal volcanic activity cycles show that eruptive fissures are more likely to open at lower altitudes and outside of the Enclos towards the end of superficial cycles, and particularly voluminous effusive events may be expected just after the peak in a deep-seated cycle. However, such atypical low flank and high-volume events are difficult to predict and can therefore be of high risk.

## 2. Methods and data

### 2.1 Digital Elevation Models

320 Given the sensitivity of lava flow paths to topography (Favalli et al., 2005), for a target where the topography changes so often as is the case at Piton de la Fournaise, using a frequently updated Digital Elevation Model (DEM) is essential for short term lava flow hazard assessment. In this study we used the most recent DEMs to build the volcano hazard map. However, because we dispose of three DEMs produced at different time we could also build and compare three hazard maps of the Enclos area for the three different time periods between 1997 and 2016. The first DEM was obtained in 1997 for the whole island as derived from from Structure From Motion analysis of (i.e., application of stereophotogrammetry) of aerial photographs acquired during the 1997’s campaign of the National Geographic Institute (IGN – which since 2012 has been named the National Institute of Geographic and Forest Information). This DEM has a 25 m horizontal resolution, and was available on a local projection (Gauss-Laborde Réunion) where elevations were based on the ellipsoid (Villeneuve, 2000). The second

330 DEM was acquired in 2008-2009 by the IGN via airborne Light Detection And Ranging (LIDAR) and has a 5 m resolution over the whole island, and 1 m resolution near the coast. The vertical resolution is 0.05 to 0.1 m (Arab-Sedze et al., 2014). This DEM was resampled at 5 m resolution across the entire island, was released in 2010 and it is hereafter referred to as the

Supprimé: and

Supprimé:

Supprimé:

Supprimé: to

Supprimé: occurring

Supprimé: mean

Supprimé: that

Supprimé: such

Supprimé: of such

Supprimé: are characterized by such “atypical”, low flank events

Supprimé: where they typically occur

Supprimé: This

Supprimé: cyclic activity

Supprimé: s

Supprimé: Digital Elevation Models

Supprimé: ¶

Mis en forme : Titre 1

Mis en forme : Retrait : Première ligne : 1.27 cm

Supprimé: , and indeed up-to-date,

Supprimé: For

Supprimé: could use to three

Supprimé: analyse

Mis en forme : Police :Italique

Mis en forme : Police :Italique

Supprimé: SIR-C images

Supprimé: vertical and

Supprimé: of 0.15 m and 25 m, respectively

“LIDAR DEM from IGN – released in 2010”. Finally, the most recent DEM was obtained in April 2016 from optical Pléiades satellite images acquired in Stereo Triplet mode and processed by the *French Centre National d’Etudes Spatiales* using their S2P restitution code (de Franchis et al., 2014). This DEM is restricted to the Enclos, which is where all topographic changes took place between 2009 and 2016. Although the resolution was 50 cm, it was resampled at 5 m for this study.

## 2.2 Lava flow recurrence time

As a first step in building our lava flow hazard map, we need to estimate lava flow recurrence times on the volcano flanks. To do this, we prepared a complete, exhaustive and statistically robust eruption inventory (cf. Peltier et al. 2021). For Piton de la Fournaise, the inventory of all historical eruptions starts at the beginning of the 18<sup>th</sup> century with the first confidently dated eruption in 1708 and can be built using the detailed chronologies in (Michon et al., 2013; Morandi et al., 2016; Villeneuve and Bachèlery, 2006). By compiling these studies and convolving them with the record maintained since establishment of the OVPF (Peltier et al., 2009; Roult et al., 2012; Vlastélic et al., 2018), as well as recent OVPF reports (ISSN 2610-5101), we estimate that Piton de la Fournaise had about 250 eruptive events over a period of three centuries. This inventory is given in Table S1.

To produce the lava flow hazard map, we need to account for recurrence of individual lava flow fields and not the number of eruptive events. This is because an eruptive event may produce several lava flow fields that can be located several kilometers apart. Therefore, an individual flow field is counted as a discrete entity and entered into the database when it is either temporally or spatially separated from another flow field. Note that in the case of a fissure opening perpendicular to the slope, the lava may erupt uniformly along the fissure to feed several lava flow units simultaneously to form a flow field of many lava fingers (cf. Kilburn and Lopes, 1988; 1991; Harris and Neri, 2002). In such a setting we counted only the main, longest flow, and do not consider all fingers that comprise the compound lava flow field in the database (e.g. Walker, 1973). In the case where there is a pause in the eruption and new flows are emitted in a second phase of activity, then the main flow produced after the hiatus is also counted. Finally, if an eruption simultaneously feeds lava flows at multiple, spatially distinct locations, each lava flow site is counted as a separate unit. Following this counting strategy, one eruption may therefore be associated to several lava flows. Since the creation of OVPF (late-1979) until the end of 2019, a period when the volcano has been continuously monitored so that the inventory can be trusted to be 100 % complete, the volcano erupted 77 times within which we can identify 128 distinct lava flows (Table S1). This translates to around 1.7 lava flows per eruption.

Given the fact that lava flows are more frequent in the Enclos than beyond its limit, we had to count the number of lava flows inside the Enclos based on a different period than for the flows outside of the Enclos. For this, we divided the volcano into five regions: the Enclos, and the *Hors Enclos*, which was sub-divided into northeast flank (NE), southeast flank (SE) and the highlands along the N120 rift zone (N120; Fig. 2a) and the rest. Inside the Enclos, we consider a time period since 1931 (the date since which a rigorous record and mapping has been possible; Derrien, 2019). Until the end of 2019, this involved a total of 193 individual lava flows (Fig. 2a; Table 1; Table S1). The recurrence time of lava flows within the Enclos

- Supprimé: , and
- Supprimé: resolution
- Supprimé: 3
- Supprimé: ,
- Supprimé: we needed to
- Supprimé: , to estimate lava flow recurrence time on the volcano flank. T
- Supprimé: since record allows (
- Supprimé: since
- Supprimé: has been detailed by several studies
- Supprimé: )
- Supprimé: has been detailed by several studies
- Supprimé:
- Supprimé: and the exhaustive record since
- Supprimé: About 95 % of these have occurred inside the Enclos (Table S1).
- Supprimé: lava flows
- Supprimé: . Moreover,
- Supprimé: Therefore, an individual flow is counted when it is either temporally or spatially separated from another flow.
- Supprimé: is counted
- Supprimé:
- Supprimé: For any eruption at Piton de la Fournaise
- Supprimé: a
- Supprimé: typically
- Supprimé: s
- Supprimé: magma
- Supprimé: s
- Supprimé: overlapping flow units
- Supprimé: case
- Supprimé: a
- Supprimé: single
- Supprimé: , the longest
- Supprimé: units
- Supprimé:
- Supprimé: longest
- Supprimé: ,
- Supprimé: so that the eruption has two flows associated with it in the data base.
- Supprimé: s
- Supprimé: 195

is therefore estimated at one every ~5.4 months for the 1931-2019 period. Over this period, only three eruptions occurred  
430 outside of the Enclos, and six lava flows were counted for these three events (three in 1977, two in 1986 and one in 1998). To  
calculate the recurrence time of *Hors Enclos* lava flows, six is a rather small number if we are to ensure a good statistical  
representation. We therefore increased the time period to extend back to 1708. Over the 1708–2019 period, fifteen lava flows  
were registered outside the Enclos (Fig. 2b; Table 1; [Table S1](#)). Nine lava flows occurred on the southeast flank of the volcano.  
Of these, five were witnessed by inhabitants (in 1774, 1776, 1800 and two in 1986), one was dated at  $80 \pm 35$  BP using  $C^{14}$   
435 dating on the carbon in the soil below the Piton Raymond lava flow (Vergniolle and Bachèlery, 1982), and three other flows  
were dated at 1726, 1765 and 1823 by measuring the base diameter of pioneer trees (Albert et al., 2020). On the northeast  
flank, we counted five flows that were all witnessed (one in 1708, three in 1977 and one in 1998). Within the less active N120  
rift zone, the number of historical eruptions is not large. According to Morandi et al., (2016), eleven tephra or lava flow deposits  
can be dated since  $2920 \pm 30$  BP, but only one lava flow has been dated after 1708 (Fig. 2b; Table 1; Table S1). This eruption  
440 (named Piton Rampe 14) was dated by  $C^{14}$  at  $140 \pm 90$  BP (Vergniolle and Bachèlery, 1982; Morandi et al., 2016). However,  
this eruption was not observed and has not been further studied. Another recent eruption is also suggested from some poorly  
characterized deposits (lapilli) close to the Trouis Blancs area at  $145 \pm 30$  BP (Morandi et al., 2016), but no lava flow has been  
identified associated with this event. However, if we consider only the one lava flow at Piton Rampe 14 since  $140 \pm 90$  BP, or  
the eleven eruptions since  $2920 \pm 30$  BP, up to now, the eruption recurrence time does not vary significantly (one every 263  
445 years and one every 209 years for the two periods, respectively). We therefore assume just one eruption over our 311-year  
period (1708-2019) of records for the N120 rift zone.

Overall, this inventory represents a minimum bound on eruptive activity because it is possible that other eruptions  
and lava flows were not observed nor have yet been identified in the geological record or dated. The minimum recurrence of  
*Hors Enclos* lava flows since 1708 is therefore estimated at one every ~21 years (Table 1). The relative occurrence probability  
450 is thus calculated by normalizing the number of lava flows per year within each region over the given period. The resulting  
relative probability of occurrence during the next eruption for a lava flow is 97.8% inside the Enclos and 2.2% outside of the  
Enclos. Beyond the Enclos relative probability can be divided into 1.4, 0.7 and 0.2% for the southeast, northeast and N120  
rift zones, respectively (Table 1).

### 2.3 Probability of vent opening

455 DOWNFLOW has been previously applied to produce lava flow hazard maps at Mount Etna (Favalli et al., 2009c,  
2011), Nyiragongo (Chirico et al., 2009; Favalli et al., 2009b), Mount Cameroon (Favalli et al., 2012), and Fogo (Richter et  
al., 2016). We here follow the same methodology developed since (Favalli et al., 2009c) and assume that future vents are more  
likely to open in areas where previous vents cluster. The probability of future vent opening is therefore determined on the basis  
of location of historical vents but must be scaled to the lava flow recurrence probability within each region (cf. sect. 3), under  
460 the general assumption that the characteristics of future eruptions will be similar to those of past eruptions.

Supprimé: Tabler  
Supprimé: observed  
Supprimé: ).  
Supprimé: A sixth  
Supprimé: event  
Supprimé: F  
Supprimé: other  
Supprimé:  
Supprimé: observed on the northeast flank

Supprimé: 311

Supprimé: the  
Supprimé: of Table S1

Supprimé: 9  
Supprimé: 9  
Supprimé: 01  
Supprimé: 29  
Supprimé: 67  
Supprimé: 0  
Supprimé: 4  
Mis en forme : Retrait : Première ligne : 1.27 cm

Supprimé: and



Our inventory of vents for Piton de la Fournaise (Table 2, Fig. 3a) is based on the mapped scoria cone distribution (Davoine and Saint-Marc, 2016; Michon et al., 2015; Di Muro et al., 2012; Villeneuve and Bachèlery, 2006) and is here updated with all new vents formed between 2015 and the end of 2019 (Fig. 3a). We counted any scoria cone that is morphologically noticeable (even undated old scoria cones) and the source point of every mapped lava flow even if they are not visible anymore but buried by more recent lava flow. This method implies that the number of vents over the entire volcano is much higher (726, Table 2) than that of the lava flow considered (208, Table 1). Inside the Enclos, for the period post-1931 (Table 3); we did not consider undated scoria cone but, in some places, we counted more than one scoria cone along a fissure although only one lava flow formed. This therefore also results in higher number of vents than that of lava flows (Table 3). Conversely in the summit craters, we were not able to properly locate all the vents but could map and count the number of flows and thus this resulted in an underestimated number of vents.

The vent density distribution (number of vents per unit area) was then obtained by applying a symmetric Gaussian smoothing kernel to the map of vent locations (Bowman and Azzalini, 2003; Favalli et al., 2012; Richter et al., 2016), with a bandwidth that is a function of the local vent density. Within the Enclos, the highest concentration is located to the southeast of the summit crater and is up to 51 vents per km<sup>2</sup>. To the east, the concentration decreases from 8 vents per km<sup>2</sup> in the Enclos Fouqué caldera, to 3 and 0.5 vents per km<sup>2</sup> in the Grandes Pentès, and the Grand-Brûlé, respectively. Outside of the Enclos, resulting vent densities range from 0.01 to 8 vents per km<sup>2</sup> in the rift zones, with a highest concentration of up to 21 vents per km<sup>2</sup> within the PRVA (as already noted by Michon et al., 2015).

We find that, of the 726 mapped vents, 45 % (327) are within the Enclos, while 55 % (399) are outside of the Enclos. For the Hors Enclos vents, 20% (142) are on the N120 rift zone, 13% (98) are on the southeast flank, 7% (49) are on the northeast flank, and 15% (110) are elsewhere on the volcano flanks (Table 2). These distributions of vents per region differ significantly from the lava flow relative occurrence probability per region (Table 1). For example, while the N120 rift zone accounts for 20% of the total number of vents (Table 2), only 0.2 % of the lava flows recorded since 1708 have occurred in this region (Table 1). Instead, within the Enclos, where ~98 % of the lava flows have been emplaced (Table 1), we count only 45 % of the total number of vents (Table 2). This difference is mainly due to the period of time required for cones located in the various regions to disappear. In the Enclos, resurfacing processes and landscape changes, such as fissure opening, building of new scoria cones over old ones and burial by lava flows occurs at much higher rates than beyond the Enclos. Therefore, the lifespan of scoria cones (vents) within the Enclos is considerably shorter than compared to that of scoria cones outside of the caldera, where 65.8 % of the Enclos has been resurfaced at least once since 1931. Moreover, the selected time period (1708-2019) does not cover the full variability in eruption location and activity cycles documented by geological studies (Morandi et al., 2016 and references therein), where (in the geologic past) eruptions outside of the Enclos have, at times, been much more frequent than during the last 300 years. For this reason, the sum of probability density function for future vent opening within a given region of the volcano was set equal to the relative occurrence probability of lava flow in that region, while the spatial distribution for future vent opening within each region follows the vent distribution itself.

**Supprimé:** Finally, any vents that were missing from this data base but were apparent from the mapping of Derrien (2019) were added.

**Supprimé:** 19.6

**Supprimé:** .5

**Supprimé:** 6.

**Supprimé:** .1

**Supprimé:** 19.6

The resulting map of the probability density function of vent opening per unit area is given in Figure 3b. The highest probabilities exceed 10 %/km<sup>2</sup> with a maximum of 24 %/km<sup>2</sup> at the summit crater and across the proximal area of the terminal shield, while moderate values are obtained across the Grandes Pentes and in the Grand-Brûlé (0.01–0.5 %/km<sup>2</sup> and 0.003–0.01 %/km<sup>2</sup>, respectively, Fig. 3b). The northeast and southeast rift zones also have low to moderate values (0.003–0.5 %/km<sup>2</sup>), while the N120 rift zone has a value of less than 0.003 %/km<sup>2</sup>. For the rest of the volcano the probability of vent opening is very low, being less than 0.0001 %/km<sup>2</sup>. However, we note an area of relatively high values (up to 0.5 %/km<sup>2</sup>) located at the PRVA (Fig. 3b).

#### 2.4 DOWNFLOW model calibration

Lava flows are gravitational flows that follow approximately the steepest descent path defined by the underlying topography (Harris, 2013). DOWNFLOW is a numerical code that computes a number ( $N$ ) of steepest descent paths from a given point over a DEM that is modified by randomly applying at every pixel a vertical perturbation in the range of  $\pm \Delta h$  (Favalli et al., 2005). By iteration over  $N$  runs, the code computes whether a pixel is hit by a lava path or not. The result of a simulation represents the probabilistic estimation of the lava flow inundation area for the given  $\Delta h$ ,  $N$  and DEM, regardless of the lava properties. Thus, before applying DOWNFLOW to a given case, the key input parameters  $\Delta h$  and  $N$  need to be defined for the volcano and DEM in question (e.g., Favalli et al., 2012; Richter et al., 2016). Calibrating DOWNFLOW therefore consists of finding the parameters  $\Delta h$  and  $N$  for a given DEM that are able to best fit the model-generated and actual lava flow areas (Favalli et al., 2005). To do this at Piton de la Fournaise, a range of  $\Delta h$  (0 to 5 m) and  $N$  (100 to 10000) were applied to selected Java flows. For each DEM, the lava flows were selected if they occurred on the unmodified DEM (i.e. the underlying topography is known). DOWNFLOW then computes the array of steepest descent paths out to the limit of the DEM, which, in our case, is the coast, but does not allow computation of lava flow lengths. Therefore, for the calibration, the simulations were cut at the actual length of the flow under consideration (Fig. 4). Following previous studies (e.g. Favalli et al., (2009b) and Richter et al. (2016)), the best fit parameters can be found by comparing the actual, mapped, lava flow area ( $A_R$ ) with that generated by the simulation ( $A_S$ ):

$$\mu = \frac{A_S \cap A_R}{A_S \cup A_R} \quad (1)$$

Under this condition,  $\mu$  is a measure of the “goodness of fit” between simulated and actual parameters, where  $\mu = 1$  then the two areas coincide perfectly and if  $\mu \rightarrow 0$  the simulation becomes increasingly unrealistic. Best fit parameters are usually obtained for  $\mu \cong 0.5$  (Tarquini and Favalli, 2011). Proietti et al. (2009) and Spataro et al. (2004) evolve this approach slightly by considering a fitting function of  $e_1 = \sqrt{\mu}$ . This yields the same results, but gives numerical values closer to one.

We performed three calibrations, one for each of the three available DEMs (Figure 4). In total, we ran 70,000 simulations. For the calibration based on the 1997 DEM, that has a resolution of 25 m, we selected the five flows that were

- Mis en forme : Retrait : Première ligne : 1.27 cm
- Supprimé : 0.5...0.5 0.003 ... [3]
- Supprimé :
- Supprimé : 5
- Supprimé : N
- Supprimé : N
- Mis en forme : Retrait : Première ligne : 1.27 cm
- Supprimé : the ...teepst descent pathss ... [4]
- Supprimé : and
- Supprimé : while ...hat is modified by randomly randomly ... [5]
- Supprimé : a given range of
- Supprimé : (...f  $\pm \Delta h$ ) ...at every pixel of the DEM ...ADDIN CSL\_CITATION ({citationItems"({{id": "ITEM-1", "itemData": {"DOI": "10.1029/2004GL021718", "ISSN": "00948276", "abstract": "A stochastic model, named DOWNFLOW, is presented to forecast possible lava flow paths with the aim of hazard assessment and mitigation. The model relies on the fact that lava flow emplacement is, in many cases, controlled by topography. The potential inundation area of the flow is determined by considering a number of steepest paths over stochastic perturbations of the original topography. Since the code requires very short computational time and few input data the model proved to be a very useful tool to obtain real-time predictions during the initial phase of an eruption. The necessary topographic information can be obtained by photogrammetry, radar altimetry, or laser scanning techniques. DOWNFLOW has been successfully applied to a number of flows, including the September 2004 lava flow, where updated topographies were available."}, "author": [{"dropping-particle": "", "family": "Favalli", "given": "Massimiliano", "non-dropping-particle": "", "parse-names": false, "suffix": ""}, {"dropping-particle": "", "family": "Pareschi", "given": "Maria Teresa", "non-dropping-particle": "", "parse-names": false, "suffix": ""}], "dropping-[6]
- Supprimé :
- Supprimé : In the present work, for the purpose of compiling ... [7]
- Supprimé :
- Mis en forme : Police : Non Gras, Non Italique
- Supprimé : the ...elected first ...ava flows. For each DEM, the [8]
- Supprimé : ir
- Supprimé : occurred immediately after the date of DEM... ... [9]
- Supprimé : If...this ratio ( ... [10]
- Supprimé : ) is one ...then the two areas coincide perfectly and [11]
- Supprimé : the ratio trends towards zero ...he simulation becom[12]
- Déplacé (insertion) [5]
- Supprimé : fitness function,
- Supprimé : (Spataro et al., 2004; Proietti et al., 2009) In order [13]
- Déplacé vers le haut [5]: fitness function,  $e_1 = \sqrt{\mu}$  (Spataro et
- Supprimé : and found that input parameters are slightly differ[14]

765 ~~erupted between 1998 and 2007~~ were considered and we obtained a best fit of  $\mu = 0.50$  for  $N > 6000$  and  $\Delta h > 4$  m. For the  
 calibration based on the 2010 and 2016 DEMs ~~that were both set at 5 m pixel resolution~~, we considered four and six flows  
 between 2010–2015 and 2016–2019, respectively (~~emplaced on the unmodified topography~~). The best fit was ~~obtained at~~  $\mu =$   
 0.54 and  $\mu = 0.51$ , respectively, for  $N > 5000$  and  $\Delta h$  of around 2 m (Fig. 4). ~~Note that the difference in DEM resolution (25~~  
 770 ~~m for 1997 and 5 m for 2010 and 2016) implies that the random noise in elevation ( $\Delta h$ ) is applied on a different spatial~~  
~~frequency. On a given topography, the lower the pixel size the more random noise is applied.~~ This means that for lower  
 resolutions we expect that the best fit is obtained for higher values of  $\Delta h$ . The calibration parameters chosen to run  
 DOWNFLOW and build the hazard maps were ~~then~~  $N = 10,000$  for all DEMs and  $\Delta h = 5$  m for the 1997 DEM and  $\Delta h = 2$  m  
 on both the 2010 and 2016 DEMs. ~~The difference in  $\Delta h$  is either due to the DEM resolution as well as to the flow dimensional~~  
~~characteristics as discussed below (see discussion).~~

Supprimé: from

Supprimé: to

Supprimé: ,

Mis en forme : Police :Non Gras, Non Italique

Mis en forme : Police :Non Gras, Non Italique

Mis en forme : Police :Non Italique

## 2.5 Lava flow length

775 To properly evaluate the probability of lava flow inundation, an estimate of expected lava flow lengths is required.  
 Several methods exist to estimate the most likely length of a lava flow. For example, at Etna Favalli et al. (2005) observed a  
 linear relationship between the altitude of the main vent and the maximum possible length of the associated flow. Another  
 method is based on the empirical relationship between the average effusion rate during an eruption and the length of the flow  
 (Walker, 1973). Alternatively, expected cooling-limited flow lengths can be calculated using a thermo-rheological model, such  
 780 as FLOWGO (Harris and Rowland, 2001), that use theoretical flow cooling and crystallization properties to estimate the point  
 at which forward motion is no longer rheologically possible (Rowland et al., 2004; Wright et al., 2005). Here, at Piton de la  
 Fournaise no clear relationship was found between lava flow length and vent elevation. Due to the great changes in slope  
 within the Enclos ( $<3^\circ$  in the Enclos Fouqué to  $35^\circ$  in the Grandes Pentés area), and the presence of deep valleys on the volcano  
 flanks, no clear relation was found between effusion rate and lava flow run out ~~lengths~~ as calculated with the FLOWGO model.  
 785 Given the high number of lava flows, it is instead possible to compute ~~the probability that a pixel at a given distance from the~~  
~~vent will be hit by lava from~~ the lava flow length frequency distribution of the historical flows. To generate this, we measured  
 the ~~long axis (as a proxy for the length)~~ of all counted lava flows (Fig. S1). ~~Inside the Enclos, the lava flow length distribution~~  
~~frequency is obtained for all the known mapped flows since 1931 and~~ until 1997, 2010 and 2016, as well as until the end of  
 790 2019 (Fig. 5a). For the *Hors Enclos* lava flows, we extended the database to all flow units that have been mapped by Bachèlery  
 and Chevallier (1982), even if they are not dated, which gave us a total of 43 lava flows to work with (see also Di Muro et al.,  
 2012; Principe et al., 2016; Fig. 5a, Fig. S1). ~~For each relevant time period, the number of lava flows reaching a given length~~  
~~is then converted into~~ a lava flow length probability distribution in %/km. ~~From this, the probability for a point downslope at~~  
 a certain distance from a vent, ~~to be reached by lava,~~ is calculated (Fig. 5b).

Supprimé: 6

Mis en forme : Retrait : Première ligne : 1.27 cm

Supprimé: a function

Supprimé: that represents

Supprimé:

Supprimé: emplaced within the Enclos since 1931

Supprimé: ,

Supprimé: and produced functions relevant for each DEM, i.e.,

Supprimé: of time

Supprimé: T

Supprimé: ,

Supprimé: f

Supprimé: which

Supprimé: a

Supprimé: function

Supprimé: to be reached by lava,

Supprimé: and

Supprimé: to a lava flow length probability distribution in %/ km,

Supprimé: for the relevant period of time

## 815 **2.6. Building probabilistic lava flow hazard maps**

A lava flow hazard map gives the probability, at each point, of inundation by the lava upon the occurrence of the next effusive eruption (Rowland et al., 2005; Wright et al., 2008). To produce a hazard map, DOWNFLOW was run at each vent of a 100-m spaced grid of computational vents. For the whole Piton de la Fournaise edifice, this represents a total of 126,000 simulations, of which 12,000 were inside the Enclos. This resulting database of simulations is an inundation matrix (or mask) defined as  $P_{ij}$ , where  $P_{ij}=1$  if the pixel  $i$  is hit, according to DOWNFLOW, by a lava flow originating from vent location  $j$  and  $P_{ij}=0$  otherwise (irrespective of the distance between  $j$  and  $i$ ). The hazard at any pixel  $i$ , with a given size  $\Delta x$  and  $\Delta y$ , is defined as the total probability  $H_i$  that the pixel  $i$  may be inundated by lava originating at any possible vent location  $j$  and is given by (Favalli et al., 2012):

$$H_i = \sum_j \rho_{vj} \Delta x \Delta y \cdot P_{ij} \cdot P_{Lij}, \quad (2)$$

825 where the sum extends over all possible vent locations  $j$  with the coordinates  $x_j$  and  $y_j$  and  $\rho_{vj}$  is the probability density function of vent opening at location  $j$  (this is shown for the whole edifice in Fig. 3b) and  $P_{Lij}$  is the probability that a lava flow originating from vent  $j$  reaches pixel  $i$  along the calculated flow path (see section 2.5; black curve in Fig. 5b).

Using this methodology, we produced the hazard map for the entire volcano and three hazard maps of the Enclos area only, one for each of the DEMs (that is in 1997, 2010 and 2016).

830 To be as up-to-date as possible, the hazard map for the entire volcano was derived using a combination of the 2016 DEM for the Enclos area and the 2010 DEM for the rest of the volcano (Fig. 6). We can do this, because the 2010 DEM will not have been affected by topographic change outside of the Enclos. We run DOWNFLOW using the best fit parameters as determined for the 2016-2019 period (Fig. 4c). In the Enclos, the lava flow length distribution was determined over 1931-2019, while for rest of the volcano, we considered the length of the flow units mapped by Bachèlery and Chevallier (1982) (cf. 835 Sect. 7; Fig. 5, Fig. S1). This is then convolved with the probability density function of vent opening from all the historical vents presented in Figure 3b following Equation 2 (cf. Sect. 5).

To build the successive hazard maps of the Enclos, we take the appropriate data set from the time of DEM generation back to 1931 (Table 3). The data set include: (i) lava flow length probability distribution ( $P_{Lij}$ ) extracted from the lava flow length measurements (Fig. 5), (ii) the probability of future vent opening ( $\rho_{vj}$ ) that is based on vent distribution and the corresponding relative recurrence time of lava flows and (iii) the DOWNFLOW mask ( $P_{ij}$ ) made from calibration tailored to each case (Fig. 4).

Supprimé: 7

Supprimé: Probabilistic

Mis en forme : Retrait : Première ligne : 1.27 cm

Supprimé: the

Supprimé: point

Supprimé: for each DEM,

Supprimé: was defined for the whole of Piton de la Fournaise and a total of 126,000 simulations, of which 12,000 were inside the Enclos, were run using DOWNFLOW

Supprimé: From this

Mis en forme : Police :Gras

Supprimé: pixel  $i$

Supprimé:  $i$

Supprimé: , it was possible to construct the lava flow hazard map which gives the probability, at each point, of inundation by lava flow upon the occurrence of the next effusive eruption (Rowland et al., 2005; Wright et al., 2008).

Supprimé: T

Supprimé: that will be inundated by lava

Supprimé:  $i$  is thus

Mis en forme : Police :Italique

Mis en forme : Police :Italique

Supprimé: that the pixel will be inundated by a lava flow,

Supprimé: and

Supprimé: ,  $\Delta x$  and  $\Delta y$  define the pixel size

Supprimé: . The mask of the simulations obtained with DOWNFLOW is given by  $P_{ij}$ , where pixel  $i$  has the value one if inundated by a lava flow originating from vent location  $j$  and has a value of zero otherwise (irrespective of the distance between  $j$  and  $i$

Supprimé: ). Finally,

Supprimé: (in % / km

Supprimé: )

Supprimé: , and is obtained by converting the frequency distribution of lava flow length for all flows up to relevant date

Supprimé: into a probability

Mis en forme : Police :Non Gras, Non Italique, Non Exposant/ Indice

Déplacé (insertion) [1]

Supprimé: 8 Discussion  
7.1 Hazard map for the entire volcano

Supprimé: NW

Supprimé: 2010

Mis en forme : Retrait : Première ligne : 1.27 cm

Supprimé:

### 3. Hazard maps

#### 3.1 Hazard map for the entire volcano

The lava flow hazard map for Piton de la Fournaise is presented in Figure 6. The map clearly shows that, for the given data set, the highest probability of lava flow inundation for the next eruption at Piton de la Fournaise is located within the Enclos. This high probability of lava flow invasion in the Enclos is undoubtedly due to the high frequency of eruptions in comparison to the rest of the volcano. Indeed, the probability of lava inundation is calculated to be high (>1 %) for about half (47%) of the Enclos area. The probability of lava flow invasion may even reach extremely high value (>10 %) in the summit craters, and in some places of the Enclos Fouqué area (above 1800 m a. s. l.) and across parts of the Grandes Pentes. In the Grand-Brûlé area, the probability is calculated to be intermediate (up to 2 %) to low (0.1–0.5 %). We note that there is a relatively high probability (of up to 2 %) that the flows will cut the belt road in some places.

The highest probability of lava flow inundation outside of the Enclos is up to 0.5 % and is on the southeast and northeast flanks of the volcano as well as in the PRVA (Fig. 6). The less active N120 rift zone has a very low, but still non-negligible, probability of lava flow invasion (<0.01 %). Although the probability of vent opening is higher at greater altitudes (Fig. 3), the lava flow length is usually longer outside of the Enclos than it is inside (Fig. 5). This implies that outside of the Enclos the probability of lava flow inundation remains the same as distance increases from the vent, while inside the Enclos it reduces with distances from the vent (lava flow length distribution peaks at around 3000 m, Fig. 5). This means that outside of the Enclos the distribution of the probability of lava flow inundation seems to depend mostly on vent location and the preferential flow path (topography) rather than the distance from the vent.

#### 3.2 Evolution of the hazard map within the Enclos

The data set used to build the three hazard maps are presented Table 3 and show that since 1931 the number of scoria cones increased from 88 in 1997 to 186 in 2019 and the number of lava flows emitted almost doubled from 111 for the period 1931–1997, to 195 for the period 1931–2019. The percentage of vents in the summit craters versus those forming in the rest of the Enclos increased from 3.4% for the period 1931–1997, to 5.8% for the period 1931–2010 and then is roughly the same since 2010 (Table 3). The relative occurrence probability of lava flow in the summit craters (Table 3) therefore decreased from 27.9 % in 1997 to 24.1 % in 2019, reflecting that eruptions within the craters become rarer over the analyzed period, becoming non-existent since 2014.

The spatial distribution of lava flow inundation probability for the three considered period (from 1931 to 1977; 1931 to 2010 and 1931 to 2019) are presented in Figure 7. The lava flow probability inside the summit craters is not represented in figure 7 because lava emitted from a vent opening in the summit crater will become entrapped in the pit, and will not be free to flow down slopes of the Enclos. In contrast, unrealistically DOWNFLOW simulation will eventually led to an overflow of lava outside the pit craters onto the slopes of the Enclos. Therefore, we did not performed simulations from the summit pit

Supprimé: ¶  
Inside the Enclos¶

Supprimé: resulting

Supprimé: map

Supprimé: (

Supprimé: .

Supprimé: )

Supprimé:

Supprimé: , where

Supprimé: 47 % of the Enclos has a high

Supprimé: (>1 %)

Supprimé: Within

Supprimé: ,

Supprimé: in

Supprimé: , the probability is extremely high (>10 %)

Supprimé: due to the low probability of vent opening as well as the relative short lava flow length distribution (in the Enclos only 11 lava flows have reached the ocean since 1931).

Supprimé: ¶  
Outside the Enclos¶

Supprimé: 7

Mis en forme : Non Surlignage

Supprimé: Evolution of

Supprimé: h

Supprimé: s with DEM

Supprimé: Given the very high number of eruptions and the existence of three DEMs, we can compare the evolution of the lava flow hazard distribution within the Enclos with time and construction of new topography (Fig. 7). To do this we built three hazard maps, one for each of the DEMs (Fig. 7).. That is, in 1997, 2010 and 2016. For each map, we take the appropriate lava flow length distribution, relative recurrence time and vent distribution from time of DEM generation back to 1931 (Fig. 5; Table 3), with the DOWNFLOW calibration tailored to each case (Fig. 4).

Mis en forme : Retrait : Première ligne : 1.27 cm

Déplacé vers le bas [2]: (Fig. 7).

Déplacé (insertion) [2]

Supprimé: T

Supprimé: at the end of 2019

Supprimé: as in 1997 (that is around 3.4–6.1 % of the vents are within the crater,

Supprimé: ). This is important, because lava emitted from a vent opening in the summit crater will become entrapped in the pit, and

Supprimé: t

Supprimé: .

create area. Note that in Figure 6, we represented an average probability inside the summit craters based on the data of table

1.

The three maps present some common features as well as changes over time. The increasing DEM resolution in 2010 (decreasing pixel size from 25 m in 1997 to 5 m in 2010) largely improve the sharpness of the maps. This provokes the high probability areas (red to purple and blue in Figure 7) to be smaller in size in the 2010 and 2016 map than in the 1997 map. On the three hazard maps, the highest probabilities (2 to >10 %) of lava flow inundation are concentrated in above 1800-1700 m a.s.l. (i.e. Enclos Fouqué caldera), with the highest value located to the south-east of the terminal cone, along the continuation of SERZ inside the Enclos, and boarding the south wall of the Enclos (Figure 7.) Between 1997 and 2010, this southeast high probability area slightly decreases in probabilities and in size. In contrast, in the 2016 hazard map, this area shows a higher value of up to 12 % and is spread over a larger area than in 2010.

In figure 8, we represented the difference in elevation and in hazard probability between the hazard maps. The improved DEM resolution has a direct effect on the spatial distribution of the probability between 1997 and 2010, resulting in an overall lowering of the probabilities and reducing of the area coverage (Figure 8; note that on the 2010-1997 map, the noise in differences is partly due to difference in acquisition methods, cf method section and on the 2016-2010 map, the positive difference near the cost is due to the vegetation that has not been removed from the 2016 DEM). One of the main differences in the spatial distribution of lava flow probability between the 2010 and 2016 hazard maps is located at the south of the terminal shield, where the August 2015 lava flow field emplaced (see Figure 7). This lava flows field is  $35.5 \times 10^6 \text{ m}^3$  and an average thickness of 8.5 m (OVPF database, Figure 8) and affected the probability calculation by clearly lowering the value in this area. However, although in 2016 hazard map the probability of lava flow invasion was estimated to be low the 2018 lava flows emplaced exactly there. This highlights the important effect of vent opening probabilities that remains high in this region and might overcome the effect of topography.

#### 4. Discussion

According to Calder et al. (2015), uncertainties in hazard maps are mainly related to three issues:

“(i) the incompleteness and bias of the geological record and the extent to which it represents possible future outcomes; (ii) the fact that analyses based on empirical models rely on a priori knowledge of the events; and (iii) the ability of complex computational models to adequately represent the full complexity of the natural phenomena”.

Our hazard maps presented here in Figures 6 and 7 have been produced from available historical and geological records of when and where past lava inundation has occurred at Piton de la Fournaise, as well as vent location and lava flow length. The quality and detail of these records improve with time, and are better inside the Enclos than outside. Secondly, the maps are based on stochastic simulations of lava flow paths using DOWNFLOW, the reliability of which depend on the quality, and up-to-dateness of our topographic model (DEM). This is an issue at a frequently active effusive center, where emplacement of

Supprimé: ed

Supprimé: The three hazard maps for the Enclos (Fig. 7) show that the highest probabilities (2 to >10 %) of lava flow inundation are concentrated in the Enclos Fouqué area (above 1800 m a.s.l.).

Mis en forme : Titre 2

Déplacé vers le haut [1]: 8 Discussion ↕

Supprimé: ed Between the 1997 and 2010, we note the development of a high probability area to the north of the terminal shield, and a slight decrease in probabilities to the southeast. This is due to the high number of eruptions occurring to the north of the shield between 1998 and 2006 (see Fig. S2). On the 2016 hazard map, the southeast part of the Enclos Fouqué shows a smaller high probability area, but with higher values of up to 12 %. This reflects a focusing of vent opening in this area over the period 2010–2016. Figure 7 also illustrates that the hazard maps were able to predict where subsequent lava flows actually occurred. Lava flows subsequent to each map were all emplaced in high probability areas, and most of the flows did not extend onto the moderate (5 %) probability zone. The exception is the 2007 eruption that occurred at a low altitude in the Grand-Brûlé, and which represents the largest eruption of the considered period. This is the only event to have occurred in a low (<1 %) probability zone (Fig. 7). ↕

Mis en forme : Couleur de police : Texte 1

Supprimé: ↕

8 ↕

.1 Hazard map interpretationsA ↕

Mis en forme : Couleur de police : Automatique

Mis en forme : Couleur de police : Automatique

Supprimé: . These are (Calder et al., 2015):

Supprimé: ,

Supprimé: location, recurrence, and

020 new lava units causes the topography to be in a state of near-constant change. Here we thus discuss the validation of the hazard  
025 maps and the uncertainties related to their interpretation and the extent to which they are adequate in assessing risk associated  
with future eruptions.

Supprimé: of the presented maps

#### 4.1 Validating hazard mapping with recent eruptions

025 The three maps of the Enclos created for different time periods are compared with emplacement location of  
subsequent lava flows (Figure 7). In this figure it is highlighted that most lava flows occurred mostly on high probability zone  
(> 2% red zone). However, most of the flows did not necessarily extend onto the very high probability zones (>5 %, i.e. purple  
to blue Figure 7). On the 1997 hazard map, we note that the longest flows that reach the coast and the 2007 flow field emplaced  
on low probability zones (<1 %; yellow, green). Because our hazard maps are computed with a database in which only four of  
the 137 eruptions since 1931 are high volume source-related-cycle terminating events (i.e. 1931, 1961, 1986 and 2007 events),  
030 such infrequent events have a low probability and hence may happen in a low probability area. For example, it is clearly visible  
that the 2007 lava flow occurred in a low (<0.5 %) probability zone of the 1997 hazard map (Figure 7a). It is therefore important  
to recall that low probability does not mean that it cannot happen, it only means that it is less probable: i.e. it is atypical if it  
happens in a low probability area. This is a major issue in terms of risk because such atypical events have exceptionally high  
lava discharge rates (which were sustained at more than 100 m<sup>3</sup>/s over 30 days in 2007; Staudacher et al., 2009), with flows  
035 advancing rapidly (within hours of the eruption onset) cut the belt road and enter the ocean (Harris and Villeneuve, 2018a).  
As a result, they are capable of rapidly inundating large areas to cause extensive damage. They thus represent the highest risk  
effusive event at Piton de la Fournaise, but are not clearly highlighted in our hazard maps. Dedicated studies on the probability  
of occurrence of such high magnitude and intensity, but atypical, events need to be conducted, and a separate set of hazard  
maps are required to compute where and when such events are more likely to happen. Likewise, our analysis does not consider  
040 the poorly studied, but relatively recent (post-1708), long-lasting activity related to overflow from summit lava lakes, as was  
common between 1750 - 1800 and around 1850 (Michon et al., 2013; Peltier et al., 2012). Our maps are, though, applicable  
only to the most commonly effusive event scenario currently encountered at Piton de la Fournaise. However, they must be  
used and trusted with the above caveats in mind regarding the type of activity and effusive event to which they apply.

#### 4.2. Historical and geological records: representativeness of future eruptions

045 Our geographical distribution of vent density per unit area (Fig. 3b) is based on an inventory of 726 vents and includes  
pre-historic vents (scoria cones) identified in the geological record back to at least 57 ka BP (McDougall, 1971). The lava flow  
inventory and recurrence probability inside the Enclos covers a time span of 88 years (from 1931 to 2019), and outside the  
Enclos the record spans 311 years (from 1708 to 2019). Given the frequency of activity, this allows a comprehensive data set  
of 220 lava flows to be used (Table S1). These relatively long periods and large numbers of cases, mean that the hazard map,  
050 of the entire volcano produced here, provide the lava flow inundation probabilities relevant at a temporal scale spanning decades  
to centuries, and is based on a statistically robust data set. As shown in Figure 7, the lava flow inundation probability

Supprimé: 8

Supprimé: 1

Supprimé: .1

Mis en forme : Retrait : Première ligne : 1.27 cm

Supprimé: s

Supprimé: s

Supprimé:

Supprimé: future vent opening and

Supprimé: are

distribution may change over the time span of a few years. However, although precise hazard maps for such active centers need to be regularly updated for short term hazard assessment (e.g. Harris et al. 2019), the topography of the Enclos remains broadly the same (Figure 8), where the slope profile is downhill from west to east, guiding flows towards the coast. Therefore, the map presented here is reliable and trustworthy for long term land use planning and management. This includes agricultural practices, urban planning, road network planning, assignment of protected areas, park-use planning, implementation of trail networks and installation of subterranean and above ground electric, sewage and gas networks; as well as targeting of potential zones where repair and replacement will be necessary (e.g. Tsang et al., 2020). Nonetheless, although, we argue that this hazard map is trustworthy in the long term, it may not be adapted for the short term, i.e., the next few days or months and over small spatial scales, i.e., hundreds of meters. Hazard maps for other timeframes could be produced with the same methodology but with appropriated input data.

For short-term hazard assessment, given the frequent resurfacing of the Enclos, the topography may locally change significantly (Figure 8). Emplacement of new lava flow units can cause subsequent flows to advance down paths that are displaced 10s to 100s of meters over what would have been the case had the initial, pre-eruption, topography applied (Harris and Rowland, 2015). As shown in Harris et al. (2019), to accurately and precisely forecast exact lava flow paths in the short term, the topography needs to be revised after each eruption, and even during relatively long-lasting (weeks-to-months long) eruptions.

### 4.3. Accounting for spatiotemporal volcanic activity patterns

Activity at Piton de la Fournaise follows cycles that evolve over time scales of a few years to a decade or so (Derrien, 2019; Got et al., 2013; Peltier et al., 2009; Roult et al., 2012; Vlastélic et al., 2018). This cyclic eruptive pattern will control the location, intensity and magnitude of the eruptions, and hence the location, length and area of inundation of associated lava flows. Eruptive fissures tend to be closer to the summit craters (i.e., proximal eruptions are more probable) at the start of a cycle than at the end (when distal eruptions are more likely to occur). Moreover, cycle durations will depend on the magma supply rate, where the lower the supply rate the longer the cycle (Derrien, 2019). Cycles also often terminate with a relatively long-lived, high volume, and high intensity effusive event (Coppola et al., 2017; Peltier et al., 2009). Therefore, depending on the length of cycle and where, temporally, in the cycle we are, both the geographical distribution of the probability of vent opening and the length of associated flow would vary. Specific hazard maps could therefore be built based on the cycles through phases of more and less frequent activity, and as the intensity of events within each cycle wax and wane.

Piton de la Fournaise also experiences longer-duration (20-30 year-long) cycles that are related to systematic evolution in the fertility of the magma source (Vlastélic et al., 2018). Phases of increasing mantle fertility are related to increasing eruption frequency and erupted volume, as the mantle porosity increases thus promoting melt extraction. Such increasing phases of activity ultimately culminate in exceptionally voluminous, eruptions with high effusion rates, as well as summit collapse or pit-crater formation; as occurred in 1931, 1961, 1986 and 2007 (Vlastélic et al., 2018). On other volcanic centers such as Hawaii or Etna, lava flow length has been related to effusion rate and lava volume (Harris and Rowland, 2001;

Supprimé: They should therefore be

Supprimé: years,

Supprimé: G

Supprimé: of the Enclos is highly variable in the short term

Supprimé: ,

Supprimé: where e

Supprimé: emplacement of new flow units, locally, can invalidate a DEM in a matter of hours, causing subsequent flow paths impossible to replicate. Thus,

Supprimé: As shown in Figure 6, the lava flow inundation probability distribution changes over the time span of a few years. However, although precise hazard maps for such active centers need to be regularly updated, over the time span of decades to centuries, the topography remains broadly the same, where in the case considered here the Enclos has a slope profile that is downhill from east to west, guiding flow towards the coast (Fig. 6).

Supprimé: The interpretation of the hazard map may also need to vary with time as a system cycles through phases of more and less frequent activity, and as the intensity of events within each cycle wax and wane.

Supprimé: will

Supprimé:

Supprimé: Given

Supprimé: that the

Supprimé: will



120 Malin, 1980; Pinkerton and Wilson, 1994; Walker, 1973), At Piton de la Fournaise further works need to be carried out to test and quantify whether there is a relationship between lava flow length and volume and effusion rate, and if this could be related to the cyclicity (Derrien, 2019; Vlastélic et al., 2018). This could therefore be used to produce specific hazard maps depending on where, in terms of time, we are in such a longer-term source-related cycle.

#### 4.3. Uncertainties related to numerical modelling

125 The DOWNFLOW stochastic approach computes the lava flow inundation area by summing  $N$  lava flow paths for a given random vertical perturbation ( $\Delta h$ ) added to the DEM. The calibration therefore requires to find the best fit values for these two main parameters. The parameter space of Figure 4 shows that the required number of runs ( $N$ ) needed to achieve a good fit with the lava flow area ( $\mu > 0.5$ ) must, in this case, be at-least 2 000–5 000. Following Tarquini and Favalli (2013), a safe choice for  $N$  to ensure statistically robust simulations and ensure model (and output map) robustness is 10 000 in all cases.

130 The calibration for  $\Delta h$  gives different results for pre- and post-2007 cases, being 5 m and 2 m, respectively. This has two explanations. The first is simply due to the difference in the DEM resolution. The resolution is 25 m for the 1997 DEM and 5 m for the other two DEMs. The bigger is the pixel size, the higher is  $\Delta h$  expected to be. The second explanation resides in the difference of lava flow dimension characteristics. According to Favalli et al. (2005),  $\Delta h$  represents the characteristic vertical height of an obstacle that the flow can overcome. This implies that, since 2007, lava flow dimensions have changed: they must

135 have become thinner as they can now only overflow an obstacle if that obstacle is 6 m lower than prior to 2007. Indeed, the lava flows in our database are more voluminous, longer and thicker between 1997 and 2007 (mean length: 3937 m, mean volume:  $17.6 \times 10^6$  m<sup>3</sup>, mean thickness 6.4 m) than between 2008 and 2019 (mean length: 2543 m, mean volume:  $6.0 \times 10^6$  m<sup>3</sup>, mean thickness 4.4 m). This difference can be related to the cyclic activity. The period between 1997 and 2007 corresponds to end of a deep source cycle (Cycle 3 of Vlastélic et al., 2018). As a result, lavas were increasingly associated with higher

140 magma fertility and magma supply rates, to produce more voluminous flows at relatively high effusion rates. Hence, following Walker (1973) and Malin (1980) if lava flows are longer and thicker, they are able to overcome higher obstacles. However, the period after 2007 relates to the beginning of a new deep source cycle (Cycle 4 of Vlastélic et al., 2018), with lower fertility and output rates. During this period the reverse is true: flows were less voluminous, and hence shorter and thinner and able to only overcome lower obstacles. The calibration parameters used for DOWNFLOW, especially  $\Delta h$ , thus must be determined for, and then applied to, a specific period of activity if the results are to be valid with the appropriate updated DEM; and changed should there be an evolution in a cycle or eruption style.

#### 4.4 Use for hazard mitigation at Piton de la Fournaise

150 In terms of hazard mitigation at Piton de la Fournaise, our maps are intended to provide information of value in planning actions implemented by local authorities and in building resilience to future eruptions, with a focus on protection of public infrastructure. Figure 6 shows the locations of all roads and hiking trails that are the most likely to be covered by future lava flows, and the lengths of each that may need to be replaced.

- Supprimé: ,
- Supprimé: the lava length frequency distribution
- Supprimé: compute
- Supprimé: the
- Supprimé: is thus
- Supprimé: ent
- Supprimé: In addition, the collapse and pit crater formation events at the end of the cycle will strongly modify the topography in the proximal region.
- Supprimé: Because our hazard maps are based on a database whose events are dominated by "typical" eruptions (i.e., only four of the 137 eruptions since 1931 are high volume source-related-cycle terminating events), they are representative only of such typical cases and event scenarios. Therefore, the maps cannot be applied to asse[16]
- Supprimé: 1.2
- Supprimé: N
- Mis en forme : Retrait : Première ligne : 1.27 cm
- Supprimé: As discussed above, the DEM thus needs to be ... [17]
- Supprimé: DOWNFLOW
- Supprimé: a choice
- Supprimé: of
- Supprimé: s: the number of runs and the maximum range of  $\Delta h$
- Supprimé: Therefore
- Supprimé: , and this is used here to ensure model (and output map)
- Supprimé: .
- Supprimé: A
- Supprimé: 2
- Supprimé: 3
- Supprimé:
- Supprimé: 6480
- Supprimé: 49
- Supprimé: 12.5
- Supprimé: 2007
- Supprimé: 2500
- Supprimé: 3.5
- Supprimé: 3
- Supprimé: units
- Supprimé: were
- Supprimé: and thus
- Supprimé: 8
- Supprimé: 2
- Mis en forme : Retrait : Première ligne : 1.27 cm

230 For the island belt road, we show that 4.5 km of the 10 km that crosses the Enclos is in an intermediate probability (>0.5 %, Fig. 6) zone in terms of lava inundation. We also show that even if the probability is low, the probability of lava flow invasion is not negligible for several municipalities situated beyond the Enclos on the northeast and southeast flanks of the volcano (i.e., Saint-Phillipe and Sainte-Rose, Fig. 6). In terms of hiking trails, although the main trail to the summit crater is in a low probability zone, it has a very high probability of future vent opening (>2 %/km<sup>2</sup>, Fig. 3). This is because when we compute the hazard map, any pixel close to the summit (at high altitude) have a contributing area (possible vent location from which the lava path would reach the pixel in question) that is much smaller (up to 1000 times) than for a pixel that is at lower altitude. Regularly since 2014, trails inside the Enclos Fouqué have been covered by lava, as for example in July 2018 when 400 m of trail in the Enclos was buried and in February 2019 when 150-200 m of trail very close to the viewing platform for the summit crater was buried (OVPF reports, ISSN 2610-5101).

240 In the case of an imminent eruption, our hazard map will thus complement the real time information that OVPF shares with civil protection, who need to identify potential locations from where people may need to be evacuated and road sections to be closed (Peltier et al., 2020). In addition, land use plans (referred as *Plan de Prévention des Risques* in French law) at La Réunion do not currently take into account volcanic hazard. Our maps are thus also intended to aid and guide stakeholders in developing effective and comprehensive mitigation and land use plans, with the caveat that our maps are for a “typical” effusive event. Separate maps will need to be drafted in the future for atypical events (such are distal and Hors Enclos eruptions), as well as for prolonged lava lake overflow at the summit. Additionally, the presented map should be updated whenever topography changes and a new DEM becomes available. We have here provided a flexible methodology that allows for ease of up-date. In consequence, for a short-term or atypical scenario, this framework allows updating of the input data (DEMs, vent locations, flow properties) to quickly produce a probabilistic map or specific flow forecast scenario as needed.

## 250 5 Conclusion

Piton de la Fournaise is one of the most active effusive centers in the world, it being a volcano that has experienced more than one eruption a year since human settlement of the island at the end of the 17<sup>th</sup> century, and two eruptions a year since the volcano has been closely monitored by OVPF since 1979. The resulting database to calculate lava flow frequency and probability of future vent opening thus comprises more than two hundred individual lava flows emplaced within the Enclos since 1931, about fifteen lava flows emplaced outside of the Enclos since 1708 and more than seven hundred vents over the entire volcano edifice. Within the most active area of the volcano (i.e., the Enclos), a lava flow has been emitted in average every five months since 1931, thirteen of which have cut the island belt road, while beyond the caldera, an effusive event has occurred on average every twenty-one years over the last three centuries. Since 1931, two Hors Enclos eruptions (in 1977 and 1986) have caused property damage. This large database allows compilation of a statistically robust hazard assessment and production of probabilistic hazard maps for lava flow inundation.

Supprimé: see

Supprimé: see

Supprimé: in terms of lava inundation

Supprimé: is in a

Supprimé: zone in terms

Supprimé: 400

Supprimé: and

Supprimé: , and

Supprimé: this

Mis en forme : Police :Italique

Supprimé: However, we

Supprimé: 9

Mis en forme : Retrait : Première ligne : 1.27 cm

Supprimé: 207

Supprimé: 15

Supprimé: 726

Déplacé vers le bas [4]: This large data base allows compilation of a statistically robust hazard assessment and production of probabilistic hazard maps for lava flow inundation.

Supprimé: 5.3

Supprimé: 13

Supprimé: 21

Mis en forme : Police :Non Gras, Italique

Supprimé: since

Supprimé: and twelve lava flows have cut the belt road

Déplacé (insertion) [4]

Supprimé:

1285 ~~We thus present here the up-to-date~~ lava flow hazard map ~~for Piton de la Fournaise~~, with lava flow path projections  
based on the stochastic model DOWNFLOW, to identify those areas that are most likely to be impacted by lava flows during  
any future eruption, and to quantify the probability of inundation ~~in the medium to long term (decades)~~. ~~The availability of~~  
~~three DEM built in 1997, 2010 and 2016 were used to produce a series of hazard maps that evolve with time and topography~~.  
Fundamentally we stress the need for frequent update of the DEMs at such frequently active volcanoes, where topography is  
constantly evolving to influence flow path. ~~This is particularly of importance for short term lava flow hazard assessment during~~  
290 ~~ongoing eruption (days to weeks)~~. In addition, given that the ~~volcanic~~ activity follows cycles that cause the location, erupted  
lava volume, effusion rate and flow dimensions to evolve with time, both the maps and the parameters used for modelling need  
to be applied on a case-dependent basis. We here produced ~~a map that applies to the frequent typical~~ effusive events, ~~where the~~  
~~Jess frequent high-volume events would consequently extend into low probability areas~~. Dedicated studies for probability  
occurrence of such high-volume events thus need to be conducted to complete the hazard assessment. Our lava flow hazard  
1295 map methodology is, though, intended as a flexible approach that can be applied to frequently active effusive centers, producing  
up-to-date maps that can be updated as eruption conditions evolve. This is essential support for informed land-use planning,  
as well as for use in crisis response and in drafting of hazard mitigation plans ~~(cf. Coppola, 2009)~~.

Supprimé: Our

Supprimé: uses these data

Supprimé: , so as to produce a series of hazard maps that evolve with time and topography

Supprimé: s

Supprimé: apply

Supprimé: that typify the first and second phases of a cycle, but not

Supprimé: terminating

Supprimé: for all effusive scenarios

Supprimé: .

#### Supplementary material

1300 Table S1: Table of the inventory of eruptions and lava flows since 1708

Figure S1: Map of the ~~lava flow axis measurements used to extract the~~ lava flow length

Figure S2: Figure of the lava flows for each period of time ~~(1931-1966; 1972-1992; 1998-2007; 2008-2019)~~

Supprimé: ed

Supprimé: 1972-1992

Supprimé: 1998

Supprimé: 2007

Supprimé: 2010

Supprimé: 2015

Supprimé: 2016

#### Data availability

1305 All data shown in this study including the eruption inventory and GIS layers (georeferenced .shp files of the vents, fissures  
and lava flows as well as the calculated density function of vent opening and hazard maps) are freely available upon request  
at the OVPF or in the supplementary material.

#### Authors contribution

1310 MOC lead this study, wrote the manuscript and made all figures and tables. MF executed the vent probability distribution, the  
DOWNFLOW calibration and computed the hazard maps; NV wrote the DEM section; AP, ADM and NV contributed to the  
eruption inventory; AD and NV draw the lava flow outlines; PB compiled the GIS data. All authors contributed to  
implementing the discussion and to the writing of the article.

#### 1315 Acknowledgements

This research was fully funded by the Agence Nationale de la Recherche through the project LAVA (Program: DS0902 2016;  
Project: ANR-16 CE39-0009, <http://www.agence-nationale-recherche.fr/Projet-ANR-16-CE39-0009>). This is ANR-LAVA

contribution no. XX [and Laboratory of Excellence ClerVolc contribution number XX](#). We thank Patrick Bachèlery for reviewing the eruption inventory and Simone Tarquini and Hannah Dietterich for their very constructive reviews that improved this article.

**Supprimé :** . It is also a

**Supprimé :** [and IPGP contribution no. XX](#)

**Mis en forme :** Surlignage

## References

- 1340 Albarède, F., Luais, B., Fitton, G., Semet, M., Kaminski, E., Upton, B. G. J., Bachèlery, P. and Cheminée, J. L.: The geochemical regimes of piton de la Fournaise volcano (Réunion) during the last 530000 years, *J. Petrol.*, 38(2), 171–201, doi:10.1093/etroj/38.2.171, 1997.
- Albert, S., Flores, O., Michon, L. and Strasberg, D.: Dating young (<1000 yrs) lava flow eruptions of Piton de la Fournaise volcano from size distribution of long-lived pioneer trees, *J. Volcanol. Geotherm. Res.*, 401(106974), doi:10.1016/j.jvolgeores.2020.106974, 2020.
- 1345 Arab-Sedze, M., Heggy, E., Bretar, F., Berveiller, D. and Jacquemoud, S.: Quantification of L-band InSAR coherence over volcanic areas using LiDAR and in situ measurements, *Remote Sens. Environ.*, 152, 202–216, doi:10.1016/j.rse.2014.06.011, 2014.
- [Bachèlery, P.: Le Piton de la Fournaise \(Ile de La Réunion\). Etude volcanologique, structural et pétrologique, Univ. Clermont-](#)
- 1350 Ferrand II., 1981.
- Bachèlery, P. and Chevallier, L.: Carte volcano-structurale du massif de la Fournaise au 1/50 000e avec notice explicative, *Publ. Inst. Phys. du Globe Paris*, 1982.
- Bertile, W.: Des coulées volcaniques à Saint-Philippe (Mars 1986) : gestion d'une catastrophe naturelle, Edition Co., Saint-Denis, La Réunion., 1987.
- 1355 Boivin, P. and Bachèlery, P.: Petrology of 1977 to 1998 eruptions of Piton de la Fournaise, La Réunion Island, *J. Volcanol. Geotherm. Res.*, 184(1), 109–125, doi:https://doi.org/10.1016/j.jvolgeores.2009.01.012, 2009.
- Bonne, K., Kervyn, M., Cascone, L., Njome, S., Van Ranst, E., Suh, E., Ayonghe, S., Jacobs, P. and Ernst, G.: A new approach to assess long-term lava flow hazard and risk using GIS and low-cost remote sensing: The case of Mount Cameroon, West Africa, *Int. J. Remote Sens.*, 29(22), 6539–6564, doi:10.1080/01431160802167873, 2008.
- 1360 Bowman, A. W. and Azzalini, A.: Computational aspects of nonparametric smoothing with illustrations from the sm library, *Comput. Stat. Data Anal.*, 42(4), 545–560, doi:10.1016/S0167-9473(02)00118-4, 2003.
- Bretar, F., Arab-Sedze, M., Champion, J., Pierrot-Deseilligny, M., Heggy, E. and Jacquemoud, S.: An advanced photogrammetric method to measure surface roughness: Application to volcanic terrains in the Piton de la Fournaise, Reunion Island, *Remote Sens. Environ.*, 135, 1–11, doi:10.1016/j.rse.2013.03.026, 2013.
- 1365 Calder, E. S., Wagner, K. and Ogburn, S. E.: Chapter 20 Volcanic hazard maps, in *Global Volcanic Hazards and Risk*, edited by S. C. Loughlin, R. S. J. Sparks, S. Brown, S. K. Jenkins, and C. Vye-Brown, Cambridge University Press, Cambridge., 2015.

**Mis en forme :** Français

- 1370 Cappello, A., Zanon, V., Del Negro, C., Ferreira, T. J. L. and Queiroz, M. G. P. S.: Exploring lava-flow hazards at Pico Island, Azores Archipelago (Portugal), *Terra Nov.*, 27(2), 156–161, doi:10.1111/ter.12143, 2015.
- Chirico, G. D., Favalli, M., Papale, P., Boschi, E., Pareschi, M. T. and Mamou-Mani, A.: Lava flow hazard at Nyiragongo Volcano, DRC 2. Hazard reduction in urban areas, *Bull. Volcanol.*, 71(4), 375–387, doi:10.1007/s00445-008-0232-z, 2009.
- Coppola, D., Di Muro, A., Peltier, A., Villeneuve, N., Ferrazzini, V., Favalli, M., Bachèlery, P., Gurioli, L., Harris, A. J. L., 1375 Moune, S., Vlastélic, I., Galle, B., Arellano, S. and Aiuppa, A.: Shallow system rejuvenation and magma discharge trends at Piton de la Fournaise volcano (La Réunion Island), *Earth Planet. Sci. Lett.*, 463, 13–24, doi:10.1016/j.epsl.2017.01.024, 2017.
- Davoine, P. and Saint-Marc, C.: A Geographical Information System for Mapping Eruption Risk at Piton de la Fournaise., in *Active Volcanoes of the Southwest Indian Ocean. Active Volcanoes of the World.*, edited by P. Bachèlery, J.-F. Lénat, A. Di Muro, and L. Michon, Springer., 2016.
- 1380 Derrien, A.: Apports des techniques photogrammétriques à l'étude du dynamisme des structures volcaniques du piton de la fournaise, Université de Paris., 2019.
- Derrien, A., Villeneuve, N., Peltier, A. and Michon, L.: Multi-temporal airborne structure-from-motion on caldera rim: Hazard, visitor exposure and origins of instabilities at Piton de la Fournaise, *Prog. Phys. Geogr. Earth Environ.*, 43(2), 193–214, doi:10.1177/0309133318808201, 2018.
- 1385 Derrien, A., Peltier, A., Villeneuve, N. and Staudacher, T.: The 2007 caldera collapse at Piton de la Fournaise: new insights from multi-temporal structure-from-motion, *Volcanica*, 3(1), 55–65, doi:10.30909/vol.03.01.5565, 2020.
- Duffield, W. A., Stieltjes, L. and Varet, J.: Huge landslide blocks in the growth of piton de la fournaise, La réunion, and Kilauea volcano, Hawaii, *J. Volcanol. Geotherm. Res.*, 12(1), 147–160, doi:https://doi.org/10.1016/0377-0273(82)90009-9, 1982.
- 1390 Favalli, M., Pareschi, M. T., Neri, A. and Isola, I.: Forecasting lava flow paths by a stochastic approach, *Geophys. Res. Lett.*, 32(3), 1–4, doi:10.1029/2004GL021718, 2005.
- Favalli, M., Tarquini, S., Fomacai, A. and Boschi, E.: A new approach to risk assessment of lava flow at Mount Etna, *Geology*, 37(12), 1111–1114, doi:10.1130/G30187A.1, 2009a.
- Favalli, M., Chirico, G. D., Papale, P., Pareschi, M. T. and Boschi, E.: Lava flow hazard at Nyiragongo volcano, D.R.C. 1.
- 1395 Model calibration and hazard mapping, *Bull. Volcanol.*, 71(4), 363–374, doi:10.1007/s00445-008-0233-y, 2009b.
- Favalli, M., Mazzarini, F., Pareschi, M. T. and Boschi, E.: Topographie control on lava flow paths at Mount Etna, Italy: Implications for hazard assessment, *J. Geophys. Res. Earth Surf.*, 114(1), 1–13, doi:10.1029/2007JF000918, 2009c.
- Favalli, M., Tarquini, S. and Fornaciai, A.: Downflow code and lidar technology for lava flow analysis and hazard assessment at mount etna, *Ann. Geophys.*, 54(5), 552–566, doi:10.4401/ag-5339, 2011.
- 1400 Favalli, M., Tarquini, S., Papale, P., Fornaciai, A. and Boschi, E.: Lava flow hazard and risk at Mt. Cameroon volcano, *Bull. Volcanol.*, 74(2), 423–439, doi:10.1007/s00445-011-0540-6, 2012.
- Felpeto, A., Araña, V., Ortiz, R., Astiz, M. and García, A.: Assessment and modelling of lava flow hazard on Lanzarote (Canary Islands), *Nat. Hazards*, 23(2–3), 247–257, doi:10.1023/A:101112330766, 2001.

Mis en forme : Français

- de Franchis, C., Meinhardt-Llopis, E., Michel, J., Morel, J.-M. and Facciolo, G.: An automatic and modular stereo pipeline for pushbroom images, *ISPRS Ann. Photogramm. Remote Sens. Spat. Inf. Sci.*, II-3, 49–56, doi:10.5194/isprsannals-II-3-49-2014, 2014.
- Gillot, P.-Y., Lefèvre, J.-C. and Nativel, P.-E.: Model for the structural evolution of the volcanoes of Réunion Island, *Earth Planet. Sci. Lett.*, 122(3), 291–302, doi:10.1016/0012-821X(94)90003-5, 1994.
- Got, J. L., Peltier, A., Staudacher, T., Kowalski, P. and Boissier, P.: Edifice strength and magma transfer modulation at Piton de la Fournaise volcano, *J. Geophys. Res. Solid Earth*, 118(9), 5040–5057, doi:10.1002/jgrb.50350, 2013.
- Harris, A.: *Thermal Remote Sensing of Active Volcanoes: A User's Manual*, Cambridge University Press, Cambridge., 2013.
- Harris, A. J. L. and Rowland, S. K.: FLOWGO: a kinematic thermo-rheological model for lava flowing in a channel, *Bull. Volcanol.*, 63, 20–44, doi:10.1007/s004450000120, 2001.
- Harris, A. J. L. and Rowland, S. K.: Effusion Rate Controls on Lava Flow Length and the Role of Heat Loss: A Review, *Leg. Georg. P.L. Walker, Spec. Publ. IAVCEI. Eds Hoskuldsson A, Thordarson T, Larsen G, Self S, Rowl. S. Geol. Soc. London.*, 2, 33–51, 2009.
- Harris, A. J. L. and Rowland, S. K.: Lava flows and rheology, *Encycl. Volcanoes*, 2nd Ed. Eds Sigurdsson H, Hought. B, McNutt SR, Rymer H, Styx J, 2015.
- Harris, A. J. L. and Villeneuve, N.: Newspaper reporting of the April 2007 eruption of Piton de la Fournaise, part 2: framing the hazard, *J. Appl. Volcanol.*, 7, 2018a.
- Harris, A. J. L. and Villeneuve, N.: Newspaper reporting of the April 2007 eruption of Piton de la Fournaise part 1: useful information or tabloid sensationalism?, *J. Appl. Volcanol.*, 7(1), 4, doi:10.1186/s13617-018-0073-1, 2018b.
- Harris, A. J. L., Rhéty, M., Gurioli, L., Villeneuve, N. and Paris, R.: Simulating the thermorheological evolution of channel-contained lava: FLOWGO and its implementation in EXCEL, in *Detecting, Modelling and Responding to Effusive Eruptions.*, vol. 426, edited by A. J. L. Harris, T. De Groeve, F. Garel, and S. A. Carn, Geological Society, London, Special Publications., 2015.
- Harris, A. J. L., Chevrel, M. O., Coppola, D., Ramsey, M. S., Hrysiwicz, A., Thivet, S., Villeneuve, N., Favalli, M., Peltier, A., Kowalski, P., DiMuro, A., Froger, J.-L. and Gurioli, L.: Validation of an integrated satellite-data-driven response to an effusive crisis: the April–May 2018 eruption of Piton de la Fournaise., *Ann. Geophys.*, 61, doi:10.4401/ag-7972, 2019.
- Keszthelyi, L. and Self, S.: Some physical requirements for the emplacement of long basaltic lava flows, *J. Geophys. Res.*, B11, 27,447-27,464, 1998.
- Kieffer, G., Tricot, B. and Vincent, P. M.: Une éruption inhabituelle (avril 1977) du Piton de la Fournaise (Ile de la Réunion) : ses enseignement volcanologiques et structuraux, *Compte Rendu l'Academis des Sci. Paris*, 285, 957–960, 1977.
- Kolzenburg, S., Giordano, D., Di Muro, A. and Dingwell, D. B.: Equilibrium Viscosity and Disequilibrium Rheology of a high Magnesium Basalt from Piton De La Fournaise volcano ,La Réunion, Indian Ocean, France, *Ann. Geophys.*, doi:10.4401/ag-7839, 2018.
- Lénat, J.-F., Bachèlery, P. and Merle, O.: Anatomy of Piton de la Fournaise volcano (La Réunion, Indian Ocean), *Bull.*

Mis en forme : Français

- Volcanol., 74(9), 1945–1961, doi:10.1007/s00445-012-0640-y, 2012.
- Malin, M. C.: Lengths of Hawaiian lava flows, *Geology*, 8(July), 306–308, 1980.
- 1440 McDougall, I.: The geochronology and evolution of the young volcanic island of Réunion, Indian Ocean, *Geochim. Cosmochim. Acta*, 35(3), 261–288, doi:https://doi.org/10.1016/0016-7037(71)90037-8, 1971.
- Merle, O. and Lénat, J.-F.: Hybrid collapse mechanism at Piton de la Fournaise volcano, Reunion Island, Indian Ocean, *J. Geophys. Res. Solid Earth*, 108(B3), 1–11, doi:10.1029/2002jb002014, 2003.
- Merle, O., Mairine, P., Michon, L., Bachèlery, P. and Smietana, M.: Calderas, landslides and paleo-canyons on Piton de la Fournaise volcano (La Réunion Island, Indian Ocean), *J. Volcanol. Geotherm. Res.*, 189(1), 131–142, doi:10.1016/j.jvolgeores.2009.11.001, 2010.
- 1445 Michon, L. and Saint-Ange, F.: Morphology of Piton de la Fournaise basaltic shield volcano (La Réunion Island): Characterization and implication in the volcano evolution, *J. Geophys. Res. Solid Earth*, 113(3), 1–19, doi:10.1029/2005JB004118, 2008.
- 1450 Michon, L., Cayol, V., Letoumeur, L., Peltier, A., Villeneuve, N. and Staudacher, T.: Edifice growth, deformation and rift zone development in basaltic setting: Insights from Piton de la Fournaise shield volcano (Réunion Island), *J. Volcanol. Geotherm. Res.*, 184(1), 14–30, doi:10.1016/j.jvolgeores.2008.11.002, 2009.
- Michon, L., DiMuro, A., Villeneuve, N., Saint-Marc, C., Fadda, P. and Manta, F.: Explosive activity of the summit cone of Piton de la Fournaise volcano (La Réunion island): A historical and geological review, *J. Volcanol. Geotherm. Res.*, 264, 117–1455 133, doi:10.1016/j.jvolgeores.2013.06.012, 2013.
- Michon, L., Ferrazzini, V., Di Muro, A., Villeneuve, N. and Famin, V.: Rift zones and magma plumbing system of Piton de la Fournaise volcano: How do they differ from Hawaii and Etna?, *J. Volcanol. Geotherm. Res.*, 303, 112–129, doi:10.1016/j.jvolgeores.2015.07.031, 2015.
- Morandi, A., Muro, A. Di, Principe, C., Leroi, G., Michon, L., Morandi, A., Muro, A. Di, Principe, C., Leroi, G., Michon, L., 1460 Id, H. A. L., Morandi, A., Muro, A. Di, Principe, C., Michon, L., Leroi, G., Norelli, F. and Bachèlery, P.: Pre-historic (< 5 kiloyear) Explosive Activity at Piton de la Fournaise Volcano, in *Active Volcanoes of the Southwest Indian Ocean*, edited by P. Bachelery, J.-F. Lenat, A. Di Muro, and L. Michon, pp. 107–138, Springer Berlin Heidelberg, Berlin Heidelberg., 2016.
- 1465 Morin, J.: *Gestion institutionnelle et réponses des populations face aux crises volcaniques : études de cas à La Réunion et en Grande Comore*, Université de la Réunion. [online] Available from: <https://tel.archives-ouvertes.fr/tel-01199868>, 2012.
- 1470 Mossoux, S., Kervyn, M. and Canters, F.: Assessing the impact of road segment obstruction on accessibility of critical services in case of a hazard, *Nat. Hazards Earth Syst. Sci.*, 19, 1251–1263, doi:10.5194/nhess-19-1251-2019, 2019.
- Di Muro, A., Bachèlery, P., Boissier, P., Davoine, P., Fadda, P., Favalli, M., Ferrazzini, V., Finizola, A., Leroi, G., Levieux, G., Mairine, P., Manta, F., Michon, L., Morandi, R., Nave, R., Peltier, A., Principe, C., Ricci, T., Roult, G., Saint-Marc, C., Staudacher, T. and Villeneuve, N.: Evaluation de l'aléa volcanique à La Réunion. [online] Available from: [http://www.reunion.developpement-durable.gouv.fr/IMG/pdf/Rapport\\_1erephase\\_etude\\_volcan\\_web\\_cle534456.pdf](http://www.reunion.developpement-durable.gouv.fr/IMG/pdf/Rapport_1erephase_etude_volcan_web_cle534456.pdf), 2012.
- Di Muro, A., Métrich, N., Vergani, D., Rosi, M., Armienti, P., Fougereux, T., Deloule, E., Arienzo, I. and Civetta, L.: The

Mis en forme : Français

Mis en forme : Français

shallow plumbing system of Piton de la Fournaise Volcano (La Réunion Island, Indian Ocean) revealed by the major 2007 caldera-forming eruption, *J. Petrol.*, 55(7), 1287–1315, doi:10.1093/petrology/egu025, 2014.

Nave, R., Ricci, T. and Pacilli, M. G.: Perception of Risk for Volcanic Hazard in Indian Ocean: La Réunion Island Case Study, in *Active Volcanoes of the Southwest Indian Ocean: Piton de la Fournaise and Karthala*, edited by P. Bachelery, J.-F. Lenat, A. Di Muro, and L. Michon, pp. 315–326, Springer Berlin Heidelberg, Berlin, Heidelberg., 2016.

Del Negro, C., Cappello, A., Neri, M., Bilotta, G., Herault, A. and Ganci, G.: Lava flow hazards at Mount Etna : constraints imposed by eruptive history and numerical simulations, *Scientific Reports*, 3(3493), 1–8, doi:10.1038/srep03493, 2013.

Oehler, J. F., Labazuy, P. and Lénat, J. F.: Recurrence of major flank landslides during the last 2-Ma-history of Reunion Island, *Bull. Volcanol.*, 66(7), 585–598, doi:10.1007/s00445-004-0341-2, 2004.

Oehler, J. F., Lénat, J. F. and Labazuy, P.: Growth and collapse of the Reunion Island volcanoes, *Bull. Volcanol.*, 70(6), 717–742, doi:10.1007/s00445-007-0163-0, 2008.

Pallister, J., Papale, P., Eichelberger, J., Newhall, C., Mandeville, C., Nakada, S., Marzocchi, W., Loughlin, S., Jolly, G., Ewert, J. and Selva, J.: Volcano observatory best practices (VOBP) workshops - A summary of findings and best-practice recommendations, *Journal of Applied Volcanology*, 2019.

Peltier, A., Bachelery, P. and Staudacher, T.: Magma transport and storage at Piton de La Fournaise (La Réunion) between 1972 and 2007: A review of geophysical and geochemical data, *J. Volcanol. Geotherm. Res.*, 184(1–2), 93–108, doi:10.1016/j.jvolgeores.2008.12.008, 2009.

Peltier, A., Massin, F., Bachelery, P. and Finizola, A.: Internal structure and building of basaltic shield volcanoes: The example of the Piton de La Fournaise terminal cone (La Réunion), *Bull. Volcanol.*, 74(8), 1881–1897, doi:10.1007/s00445-012-0636-7, 2012.

Peltier, A., Villeneuve, N., Ferrazzini, V., Testud, S., Hassen Ali, T., Boissier, P. and Catherine, P.: Changes in the Long-Term Geophysical Eruptive Precursors at Piton de la Fournaise: Implications for the Response Management, *Front. Earth Sci.*, 6(July), 1–10, doi:10.3389/feart.2018.00104, 2018.

Peltier, A., Ferrazzini, V., Di Muro, A., Kowalski, P., Villeneuve, N., Richter, N., Chevrel, M. O., Froger, J.-L. and Hrysiewicz A, Gouhier M, Coppola D, Retailleau L, Beauducel F, Boissier P, Brunet C, Catherine P, Fontaine F, Lauret F, Garavaglia L, Lebreton J, Canjamale K, Desfete N, Griot C, Arellano S, Liuzzo M, G. S.: Volcano crisis management during COVID-19 lockdown at Piton de la Fournaise (La Réunion), *Seismol. Res. Lett.*, On line No, 1–15, doi:10.1785/0220200212, 2020.

Pinkerton, H. and Wilson, L.: Factor controlling the lengths of channel-fed lava flows, *Bull. Volcanol.*, 6, 108–120, 1994.

Principe, C., Morandi, A., Di Muro, A. and Michon, L.: Volcanological Map of the Plaine des Sables, Piton de la Fournaise, in *Active Volcanoes of the Southwest Indian Ocean: Piton de la Fournaise and Karthala*, edited by P. Bachelery, J.-F. Lenat, A. Di Muro, and L. Michon, pp. 327–330, Springer Berlin Heidelberg, Berlin, Heidelberg., 2016.

Proietti, C., Coltelli, M., Marsella, M. and Fujita, E.: A quantitative approach for evaluating lava flow simulation reliability: LavaSIM code applied to the 2001 Etna eruption, *Geochemistry, Geophys. Geosystems*, 10(9), doi:https://doi.org/10.1029/2009GC002426, 2009.



- Rh ty, M., Harris, A. J. L., Villeneuve, N., Gurioli, L., M dard, E., Chevrel, M. O. and Bach lery, P.: A comparison of cooling-limited and volume-limited flow systems: Examples from channels in the Piton de la Fournaise April 2007 lava-flow field, *Geochemistry, Geophys. Geosystems*, 18(9), 3270–3291, doi:10.1002/2017GC006839, 2017.
- Richter, N., Favalli, M., De Zeeuw-Van Dalftsen, E., Fornaciai, A., Da Silva Fernandes, R. M., P rez, N. M., Levy, J., Vict ria, S. S. and Walter, T. R.: Lava flow hazard at Fogo Volcano, Cabo Verde, before and after the 2014-2015 eruption, *Nat. Hazards Earth Syst. Sci.*, 16(8), 1925–1951, doi:10.5194/nhess-16-1925-2016, 2016.
- Roult, G., Peltier, A., Taisne, B., Staudacher, T., Ferrazzini, V., Di Muro, A. and Group, and the O.: A new comprehensive classification of the Piton de la Fournaise eruptions spanning the 1986-2011 period. Search and analysis of eruption precursors from a broad-band seismological station., *J. Volcanol. Geotherm. Res.*, 241–242, 78–104, doi:10.1016/j.jvolgeores.2012.06.012, 2012.
- Rowland, S. K., Harris, A. J. L. and Garbeil, H.: Effects of Martian conditions on numerically modeled, cooling-limited, channelized lava flows, *J. Geophys. Res.*, 109, E100101, doi:doi.org/10.1029/2004JE002288, 2004.
- Rowland, S. K., Garbeil, H. and Harris, A. J. L.: Lengths and hazards from channel-fed lava flows on Mauna Loa, Hawaii, determined from thermal and downslope modeling with FLOWGO, *Bull. Volcanol.*, 67, 634–647, 2005.
- Soldati, A., Harris, A. J. L., Gurioli, L., Villeneuve, N., Rh ty, M., Gomez, F. and Whittington, A.: Textural, thermal, and topographic constraints on lava flow system structure: the December 2010 eruption of Piton de la Fournaise, *Bull. Volcanol.*, 80(10), doi:10.1007/s00445-018-1246-9, 2018.
- Spataro, W., D’Ambrosio, D., Rongo, R. and Trunfio, G. A.: An Evolutionary Approach for Modelling Lava Flows Through Cellular Automata, in *Cellular Automata*, edited by P. M. A. Sloot, B. Chopard, and A. G. Hoekstra, pp. 725–734, Springer Berlin Heidelberg, Berlin, Heidelberg., 2004.
- Staudacher, T., Ferrazzini, V., Peltier, A., Kowalski, P., Boissier, P., Catherine, P., Lauret, F. and Massin, F.: The April 2007 eruption and the Dolomieu crater collapse, two major events at Piton de la Fournaise (La R union Island, Indian Ocean), *J. Volcanol. Geotherm. Res.*, 184(1–2), 126–137, doi:10.1016/j.jvolgeores.2008.11.005, 2009.
- Staudacher, T., Peltier, A., Ferrazzini, V., Di Muro, A., Boissier, P., Catherine, P., Kowalski, P., Lauret, F. and Lebreton, J.: Fifteen Years of Intense Eruptive Activity (1998–2013) at Piton de la Fournaise Volcano: A Review, in *Active Volcanoes of the Southwest Indian Ocean: Piton de la Fournaise and Karthala*, edited by P. Bachelery, J.-F. Lenat, A. Di Muro, and L. Michon, pp. 139–170, Springer Berlin Heidelberg, Berlin, Heidelberg., 2016.
- Tarquini, S. and Favalli, M.: Mapping and DOWNFLOW simulation of recent lava flow fields at Mount Etna, *J. Volcanol. Geotherm. Res.*, 204(1–4), 27–39, doi:10.1016/j.jvolgeores.2011.05.001, 2011.
- Tarquini, S. and Favalli, M.: Uncertainties in lava flow hazard maps derived from numerical simulations: The case study of Mount Etna, *J. Volcanol. Geotherm. Res.*, 260, 90–102, doi:https://doi.org/10.1016/j.jvolgeores.2013.04.017, 2013.
- Tsang, S. W. R., Lindsay, J. M., Kennedy, B. and Deligne, N. I.: Thermal impacts of basaltic lava flows to buried infrastructure: Workflow to determine the hazard, *J. Appl. Volcanol.*, 9(1), 1–18, doi:10.1186/s13617-020-00098-w, 2020.
- Vergnolle, S. and Bach lery, P.: R sultats de datations sur bois carbonis s pr lev s sur le massif de la Fournaise ( le de La

- 540 Réunion), Observatoire Volcanologique du Piton de la Fournaise, unpublished internal report., 1982.
- Villeneuve, N.: Apports multi-sources à une meilleure compréhension de la mise en place des coulées de lave et des risques associés au Piton de la Fournaise: Géomorphologie quantitative en terrain volcanique., Institut de Physique du Globe de Paris., 2000.
- Villeneuve, N. and Bachèlery, P.: Revue de la Typologie des Eruptions au Piton de la Fournaise, Processus et Risqué
- 545 Volcaniques Associés, Cybergegeo, doi:doi.org/10.4000/cybergegeo.2536, 2006.
- Villeneuve, N., Neuville, D. R., Boivin, P., Bachèlery, P. and Richet, P.: Magma crystallization and viscosity: A study of molten basalts from the Piton de la Fournaise volcano (La Réunion island), *Chem. Geol.*, 256, 242–251, 2008.
- Vlastélic, I., Di Muro, A., Bachèlery, P., Gurioli, L., Auclair, D. and Gannoun, A.: Control of source fertility on the eruptive activity of Piton de la Fournaise volcano, La Réunion, *Sci. Rep.*, 8(1), 1–7, doi:10.1038/s41598-018-32809-0, 2018.
- 550 Walker, G. P. L.: Lengths of lava flows, *Philos. Trans. R. Soc. London*, 274, 107–118, 1973.
- Wright, R., Garbeil, H. and Harris, A. J. L.: Using infrared satellite data to drive a thermo-rheological/stochastic lava flow emplacement model: A method for near-real-time volcanic hazard assessment, *Geophys. Res. Lett.*, 35(19), 1–5, doi:10.1029/2008GL035228, 2008.

555

Mis en forme : Retrait : Gauche : 0 cm, Suspendu : 1.25 cm

Figures and Tables:

Figure 1:

a) La Réunion island (© Google Earth) where the green line delineates the two volcanoes: Piton des Neiges (PN) to the northwest and Piton de la Fournaise (PF) to the southeast.

b) General map of Piton de la Fournaise showing the eruptive fissures as mapped up to end of 2019 (blue lines) and the buildings (in black) with the main municipalities, main roads (in brown - RN2 is the national road) and touristic trails (white lines). The main three rift zones: north 120° (N120), northeast (NERZ) and southeast (SERZ) and the two volcanic zone: Puy Raymond Volcanic Alignment (PRVA) and South Volcanic Zone (SVZ) are delineated by the dashed red lines as suggested in Bachèlery (1981) and Michon et al. (2015). The yellow contour outlines the Enclos depression that is separated in three regions by the dashed yellow lines: the Enclos Fouqué (EF), the steep slopes “Grandes Pentes” (GP) and the eastern lower part “Grand-Brûlé” (GB). The dashed yellow line between EF and GP is situated at 1800-1700 m. a.s.l. while the one between GP and GB is around 500 m. a.s.l. The background is the hill-shade of LiDAR DEM from IGN – released in 2010 and coordinates are within system WGS84-UTM 40S. Buildings, roads and trails are from BD TOPO® IGN.

Supprimé: and

Supprimé: and

Supprimé: ¶

Figure 2: Maps of the lava flows considered in this study.

a) Lava flows inside the Enclos since 1931 (date from which the lava flow mapping has been well recorded) up to end of 2019 from pale to dark red (see Derrien, 2019).

b) Lava flows outside the Enclos since 1708 and until end of 2019 including i) observed flows (pale orange to red) (see Michon et al. 2015); ii) not observed but mapped and dated lava flows (in blue and numbers indicate the year before BP for C14 dated flows – see Vergniolle and Bachèlery, 1982) and iii) tree-dated lava flows (these are not mapped but the datation location is represented by the green dots, and associated numbers indicate the calendar year for flows - Albert et al. 2020). The yellow lines represent the limits between the regions we consider. The background is the hill-shade of LiDAR DEM from IGN – released in 2010.

Supprimé: whit

Supprimé: e

Supprimé: -

Supprimé: (

Supprimé: e

Supprimé: ,

Supprimé: the

1600 Figure 3:

a) Distribution and density (in number/km<sup>2</sup>) of scoria cones (black dots) on Piton de la Fournaise based on available inventory (OVPF database). In black are scoria cones older than 1931 and in white are the vents from 1931 to the end of 2019. In total they are 726 vents. The yellow lines represent the limits between the regions we considered to estimate probability of vent opening and compute the hazards maps: the Enclos, southeast (SE), northeast (NE), and north 120° (N120) rift zones.

605 b) Probability density function of vent opening (in %/km<sup>2</sup>). The dashed lines outline the rift zones to the N 120° (N120), to the northeast (NERZ) and to the southeast (SERZ) as well as the Puy Raymond volcanic alignment (PRVA) – (Bachelery 1981; Michon et al. 2015).

1610 The background is the hill-shade of LiDAR DEM from IGN – released in 2010.

Supprimé: N

Supprimé: R

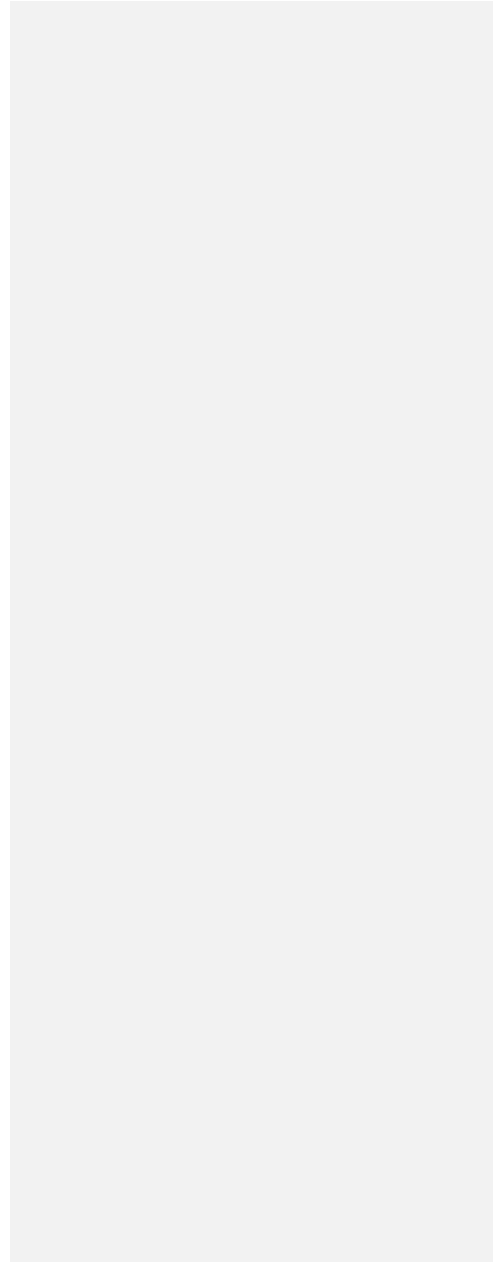
Supprimé: Z

Supprimé: The green line represents the limit of Piton de la Fournaise with Piton des Neiges.

Figure 4: DOWNFLOW calibration for a selected set of lava flows for the three time periods: a) on the 25 m resolution 1997 DEM; b) on the 2010 LiDAR DEM, c) on the 2016 DEM produced from Pleiades. To the left, the maps show the 1615 lava flow contours in red and the best DOWNFLOW simulations in blue. To the right, the best fit distribution over the  $\Delta h - N$  space (best-fit parameter range are in dark red and blue).

625 Figure 5: a) Frequency distribution of the lava flow length (by step of 500 m) at Piton de la Fournaise (La Réunion) for lava flows within the Enclos since 1931 and up to 1997, 2010, 2016 and 2019; and for all mapped flows outside the Enclos. b) Probability for a lava flow to reach a given distance (black line) and the corresponding lava flow length probability distribution (in red), for the 1931-2019 period, as function of distance from the vent.

630



635 **Figure 6: Lava flow hazard map of Piton de la Fournaise. Probability of lava flow invasion is given as percentages and is color coded from extremely low (<0.01 %) to extremely high (>10 %). The buildings are represented as black polygons, and the main roads are in brown (in bold is the RN2 national road) and touristic trails are the white lines (data from from BD TOPO® IGN). The dashed red lines outline the rift zones to the N 120° (N120), to the northeast (NERZ) and to the southeast (SERZ) as well as the Puy Raymond volcanic alignment (PRVA) – (Bachèlery 1981; Michon et al. 2015). The dashed yellow lines separate the Enclos Fouqué caldera (EF) area from the steep slopes “Grandes Pentes” (GP) at 1800-1700 m. a.s.l. and the GP from the eastern lower part “Grand-Brûlé” (GB) at around 500 m. a.s.l. The background is the hill-shade of LiDAR DEM from IGN – released in 2010.**

**Supprimé:** Black polygons and grey lines represent the buildings and roads, respectively (municipalities are indicated) and white lines are the touristic trails

**Supprimé:** The green line represents the limit of Piton de la Fournaise with Piton des Neiges.

**Supprimé:** Buildings and roads are from BD TOPO® IGN.

645 **Figure 7: Left column: Evolution of the lava flow hazard maps within the Enclos. The hazard maps are made on the DEM from 1997, 2010 and 2016, respectively, with the corresponding calibration (Fig. 4) and appropriated dataset since 1931 up to the corresponding date (Table 3, Fig. 5).**

650 **Middle column: successive annual lava flow coverage from the time of the DEM acquisition up to end of 2009 for the 1997 map and up to the end of 2019 for the 2010 and 2016 maps.**

**Right column: maps show the successive lava flows outline (as shown in the middle column) for the given time period.**

**Supprimé:** ¶

.....Saut de page.....

**Supprimé:** Evolution of the lava flow hazard maps within the Enclos.

**Supprimé:** To the left: the hazard maps are made on the DEM from 1997, 2010 and 2016, respectively, with the corresponding calibration (Fig. 4) and appropriated dataset since 1931 up to the corresponding date (Table 3, Fig. 5).

**Supprimé:** n

655 **Figure 8: Left column: difference in elevation between 1997 DEM and 2010 DEM (top) and between 2010 DEM and 2016 DEM (bottom). Note that 1) on the 2010-1997 map, the noise in differences is partly due to difference in acquisition methods (c.f. method), 2) on the 2016-2010 map, the positive difference near the cost is due to the vegetation (that has not been removed from the 2016 DEM). Right column: difference of the hazard maps (probability of lava flow invasion in %) built with the data up to 1997 and up to 2010 (top) and built with the data up to 2010 and up to 2016 (bottom).**

660

665

1685

**Table 1: Number of lava flow and statistic of recurrence and relative occurrence probability (see Table S1 for inventory).**

Region	N. lava flows	Time interval (years)	Recurrence time (year)	N. lava flows per year (year <sup>-1</sup> )	Relative occurrence probability (%)
Summit craters	47	88	1.9	0.53	23.8
Enclos w/out craters*	146	88	0.6	1.66	73.9
<b>Inside Enclos**</b>	<b>195</b>		<b>0.5 (5.4 months)</b>	<b>2.19</b>	<b>97.8</b>
SE	9	290	32.2	0.03	1.4
NE	5	311	62.2	0.02	0.7
N120	1	209	209.0	0.005	0.2
<b>Hors Enclos ***</b>	<b>15</b>		<b>20.7</b>	<b>0.05</b>	<b>2.2</b>
<b>Total</b>	<b>208</b>			<b>2.2</b>	<b>100.0</b>

\*Enclos includes the Enclos Fouqué, Grandes Pentes and Grand-Brûlé, except the summit craters area

\*\*Inside Enclos includes the whole Enclos with the summit craters. Lava flows are counted since 1931 up to the end of 2019.

1690

\*\*\*Outside Enclos lava flows are divided by region south of the caldera (SE), north (NE) and along the N120 rift zone (N120) (see Figure 2), # Time interval corresponds to the time between the oldest considered dated lava flow up to the end of 2019.

1695

- Supprimé: 87
- Supprimé: 4
- Supprimé: .
- Supprimé: 55
- Supprimé: 148
- Supprimé: 59
- Supprimé: 68
- Supprimé: 2
- Supprimé: 74
- Supprimé: 16
- Supprimé: 45
- Supprimé: 216
- Supprimé: 87
- Supprimé: 22
- Supprimé: 1
- Supprimé: 37
- Supprimé: 0
- Supprimé: 016
- Supprimé: 1
- Supprimé: 0
- Supprimé: 1
- Supprimé: 3
- Supprimé: 048
- Supprimé: 1
- Supprimé: 3
- Supprimé: 2.3
- Supprimé: 210

**Table 2: Scoria cone distribution divided by regions**

Region	N. vents	Fraction of vents (%)
Summit craters	27	3.7
Enclos w/out craters*	300	41.3
<b>Inside Enclos**</b>	<b>327</b>	<b>45.0</b>
SE	98	13.5
NE	49	6.7
N120	142	19.6
Rest of the volcano	110	15.2
<b>Hors Enclos***</b>	<b>399</b>	<b>55.0</b>
Total	726	100

Supprimé: 2

Supprimé: 2

Supprimé: 4

Supprimé: 0

Supprimé: 5

Supprimé: 56

Supprimé: 15

Supprimé: 54

Supprimé: 96

1725 \*Enclos includes the Enclos Fouqué, Grandes Pentes and Grand-Brûlé, except the summit craters area

\*\*Inside Enclos includes the whole Enclos with the summit craters. Lava flows are counted since 1931 up to the end of 2019.

\*\*\*Outside Enclos lava flows are divided by region south of the caldera (SE), north (NE) and along the N120 rift zone (N120) (see Figure 2),



**Table 3: Lava flow relative occurrence probability and scoria cone distribution within Enclos for the 1931-1997, 1931-2010, 1931-2016 and 1931-2019 periods**

Region	N. lava flows	Time interval (years)	Recurrence time (year)	N. lava flows per year (year <sup>-1</sup> )	Relative occurrence probability (%)	N. Scoria cones	Fraction of Scoria cones (%)
since 1931 up to 1997							
Summit craters	31	66	2.1	0.5	27.9	3	3.4
Enclos w/out craters	80	66	0.8	1.2	72.1	85	96.6
Total	111			1.7	100.0	88	100
since 1931 up to 2010							
Summit craters	46	79	1.7	0.6	26.7	9	5.8
Enclos w/out craters	126	79	0.6	1.6	73.3	146	94.2
Total	172			2.2	100.0	155	100
since 1931 up to 2016							
Summit craters	47	85	1.8	0.5	25.8	10	6.1
Enclos w/out craters	135	85	0.6	1.6	74.2	154	93.9
Total	182			2.1	100.00	164	100
since 1931 up to 2019							
Summit craters	47	88	1.9	0.5	24.1	10	5.4
Enclos w/out craters	148	88	0.6	1.7	75.9	176	94.6
Total	195			2.2	100.00	186	100

Supprimé: 3  
 Supprimé: 47  
 Supprimé: 3  
 Supprimé: 1  
 Supprimé: 3  
 Supprimé: 1  
 Supprimé: 07  
 Supprimé: 59  
 Supprimé: 68  
 Supprimé: 0  
 Supprimé: 2  
 Supprimé: 58  
 Supprimé: 4  
 Supprimé: 1  
 Supprimé: 3  
 Supprimé: 59  
 Supprimé: 26  
 Supprimé: 19  
 Supprimé: 18  
 Supprimé: 0  
 Supprimé: 1  
 Supprimé: 5  
 Supprimé: 2  
 Supprimé: 0  
 Supprimé: 3  
 Supprimé: 59  
 Supprimé: 18  
 Supprimé: 0  
 Supprimé: 4  
 Supprimé: 87  
 Supprimé: 3  
 Supprimé: 22.7...4.11 ... [19]  
 Supprimé: 38  
 Supprimé: 160  
 Supprimé: 5...5 ... [20]  
 Supprimé: 8...2 ... [21]  
 Supprimé: 7...929 ... [22]  
 Supprimé: 2  
 Supprimé: 2.3...25 ... [23]  
 Supprimé: 207  
 Supprimé: Figure S1 :

Page 5 : [1] Supprimé	Oryaëlle	21/04/2021 09:12:00
Page 5 : [2] Supprimé	Oryaëlle	01/06/2021 10:52:00
Page 10 : [3] Supprimé	max	22/04/2021 15:23:00
Page 10 : [3] Supprimé	max	22/04/2021 15:23:00
Page 10 : [4] Supprimé	Oryaëlle	15/03/2021 19:41:00
Page 10 : [4] Supprimé	Oryaëlle	15/03/2021 19:41:00
Page 10 : [5] Supprimé	Oryaëlle	15/03/2021 19:43:00
Page 10 : [5] Supprimé	Oryaëlle	15/03/2021 19:43:00
Page 10 : [6] Supprimé	Oryaëlle	23/04/2021 15:34:00
Page 10 : [6] Supprimé	Oryaëlle	23/04/2021 15:34:00
Page 10 : [6] Supprimé	Oryaëlle	23/04/2021 15:34:00
Page 10 : [6] Supprimé	Oryaëlle	23/04/2021 15:34:00
Page 10 : [6] Supprimé	Oryaëlle	23/04/2021 15:34:00
Page 10 : [6] Supprimé	Oryaëlle	23/04/2021 15:34:00
Page 10 : [7] Supprimé	Oryaëlle	23/04/2021 15:38:00
Page 10 : [7] Supprimé	Oryaëlle	23/04/2021 15:38:00

Page 10 : [8] Supprimé Oryaëlle 15/03/2021 21:13:00

Page 10 : [8] Supprimé Oryaëlle 15/03/2021 21:13:00

Page 10 : [9] Supprimé Oryaëlle 15/03/2021 21:16:00

Page 10 : [9] Supprimé Oryaëlle 15/03/2021 21:16:00

Page 10 : [9] Supprimé Oryaëlle 15/03/2021 21:16:00

Page 10 : [9] Supprimé Oryaëlle 15/03/2021 21:16:00

Page 10 : [9] Supprimé Oryaëlle 15/03/2021 21:16:00

Page 10 : [10] Supprimé Oryaëlle 01/06/2021 15:08:00

Page 10 : [10] Supprimé Oryaëlle 01/06/2021 15:08:00

Page 10 : [11] Supprimé Oryaëlle 12/03/2021 16:31:00

Page 10 : [11] Supprimé Oryaëlle 12/03/2021 16:31:00

Page 10 : [12] Supprimé Oryaëlle 12/03/2021 16:34:00

Page 10 : [12] Supprimé Oryaëlle 12/03/2021 16:34:00

Page 10 : [12] Supprimé Oryaëlle 12/03/2021 16:34:00

Page 10 : [13] Supprimé Oryaëlle 23/04/2021 15:47:00

Page 10 : [14] Supprimé Oryaëlle 23/03/2021 13:36:00

▼ ..... ◀  
▲ .....  
**Page 17 : [17] Supprimé** Oryaëlle 13/05/2021 09:43:00

▼ ..... ◀  
▲ .....  
**Page 17 : [18] Supprimé** Oryaëlle 13/05/2021 09:46:00

▼ ..... ◀  
▲ .....  
**Page 33 : [19] Supprimé** Oryaëlle 27/04/2021 10:14:00

▼ ..... ◀  
▲ .....  
**Page 33 : [19] Supprimé** Oryaëlle 27/04/2021 10:14:00

▼ ..... ◀  
▲ .....  
**Page 33 : [20] Supprimé** Oryaëlle 27/04/2021 10:14:00

▼ ..... ◀  
▲ .....  
**Page 33 : [20] Supprimé** Oryaëlle 27/04/2021 10:14:00

▼ ..... ◀  
▲ .....  
**Page 33 : [21] Supprimé** Oryaëlle 27/04/2021 10:14:00

▼ ..... ◀  
▲ .....  
**Page 33 : [21] Supprimé** Oryaëlle 27/04/2021 10:14:00

▼ ..... ◀  
▲ .....  
**Page 33 : [22] Supprimé** Oryaëlle 27/04/2021 10:14:00

▼ ..... ◀  
▲ .....  
**Page 33 : [22] Supprimé** Oryaëlle 27/04/2021 10:14:00

▼ ..... ◀  
▲ .....  
**Page 33 : [23] Supprimé** Oryaëlle 27/04/2021 10:14:00

▼ ..... ◀  
▲ .....  
**Page 33 : [23] Supprimé** Oryaëlle 27/04/2021 10:14:00  
▼ ..... ◀  
▲ .....